18EE8732:Micro and Nano Scale Sensors and Transducers

MODULE – 2: Motion & Acceleration Sensors

Prepared By,
Shreeshayana R
Electrical and Electronics Engineering
ATME College of Engineering, Mysuru

CONTENTS

Module-2

Motion and Acceleration Sensors: Ultrahigh Sensitivity, Wide Dynamic Range Sensors, Other Motion and Acceleration Micro sensors.

Gas and Smoke Sensors: A CO Gas Sensor Based on Nanotechnology, Smoke Detectors.

Ultrahigh Sensitivity, Wide Dynamic Range Sensors

A number of new applications, such as self-guided small projectiles and autonomous surveillance airplanes, have created a requirement for a highly sensitive yet very small acceleration sensor.

A new **miniature acceleration sensor** with a radical new design was recently introduced.

The sensor offers a very large **dynamic range and high sensitivity**.

Structure

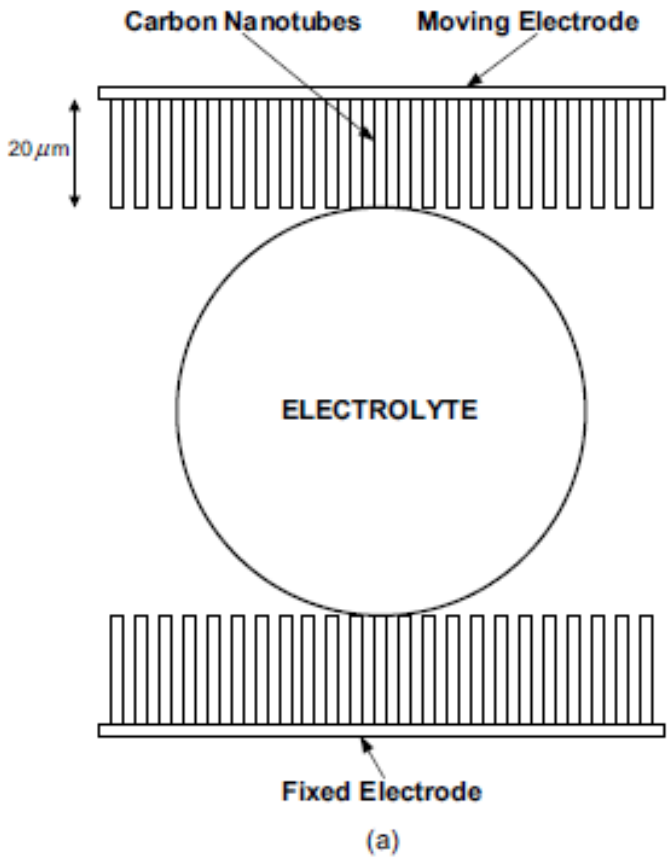

(a)

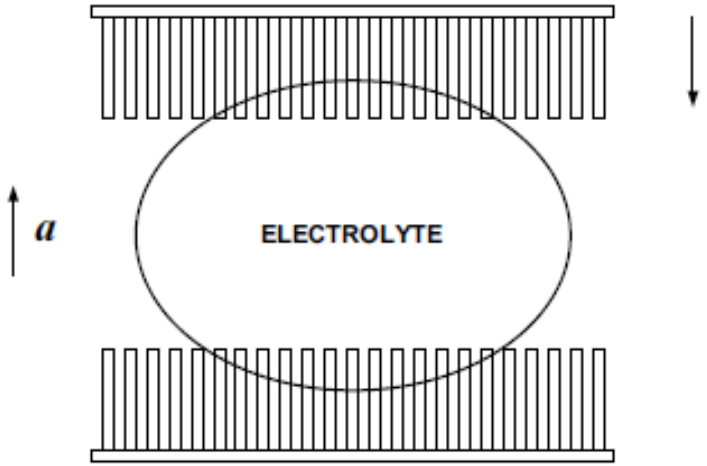

(b)

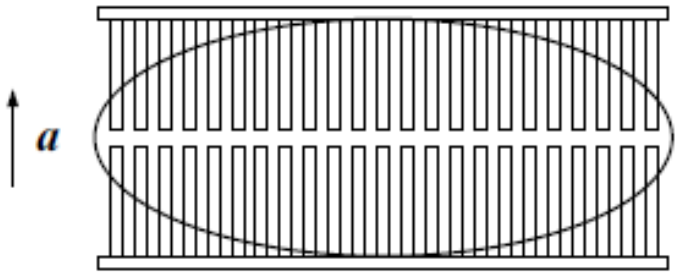

(c)

Structure

Step-1: The new acceleration sensor is based on the concept of creating a variable ultra capacitor structure that consists of one **small droplet of electrolyte** that is positioned between **two carbon nanotube (CNT) electrodes.**

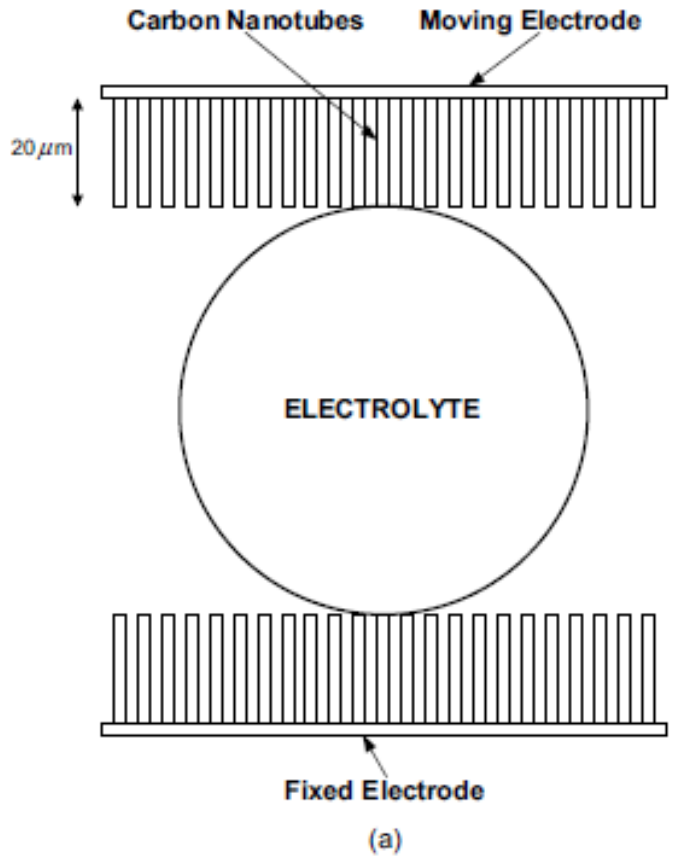

Step-2: The CNT electrodes remain outside of the electrolyte due to their hydrophobic nature.

Step-3: Under acceleration, however, **the inertial forces push the CNT electrodes into the electrolyte** and the typical capacitance of an ultra capacitor is obtained.

Structure

Step-4: Figure (a), a small droplet of electrolyte (fluid with high ionic conductivity) is placed between two electrodes on which **CNTs of a length of 20 µm are grown.**

Step-5: One electrode is fixed while the other is movable, as shown.

Step-6: Since the weights of the droplet and the electrodes are very small, and since CNTs are superhydrophobic, the CNTs **do not penetrate the electrolyte when the mechanism is at rest.**

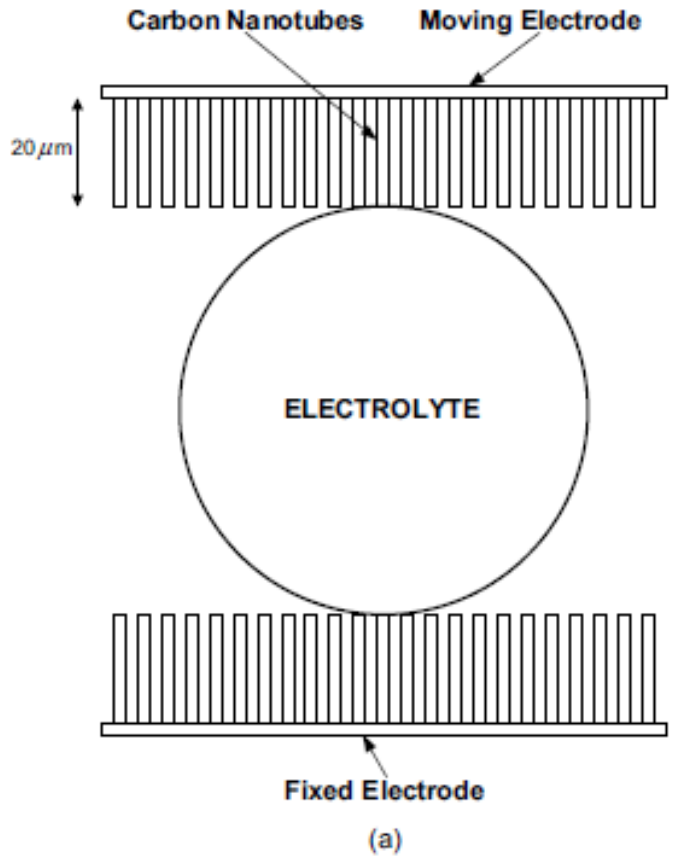

Structure

Step-7: In Figure (b), as acceleration occurs along the axis of the device (here, vertically, upward), the inertial forces created by the droplet and the moving electrode cause the CNTs to penetrate the electrolyte

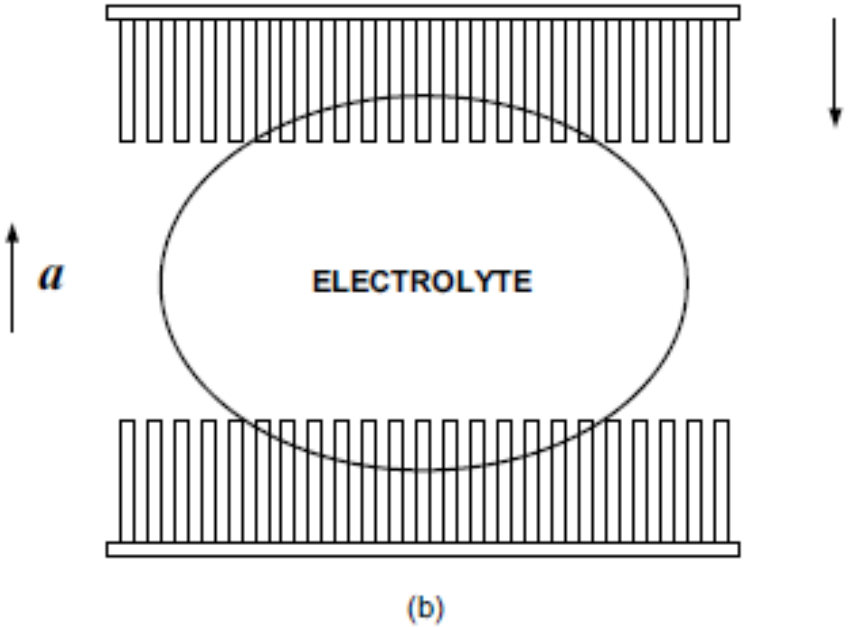

Structure

Step-8: The forces created due to inertia further increase at higher accelerations, and the penetration of the CNTs into the electrolyte **increase to a maximum.**

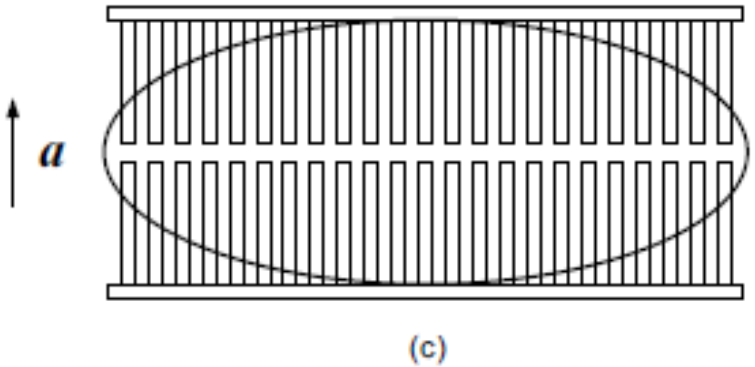

The capacitance of the thus-formed ultracapacitor increases to a substantially high value

Structure

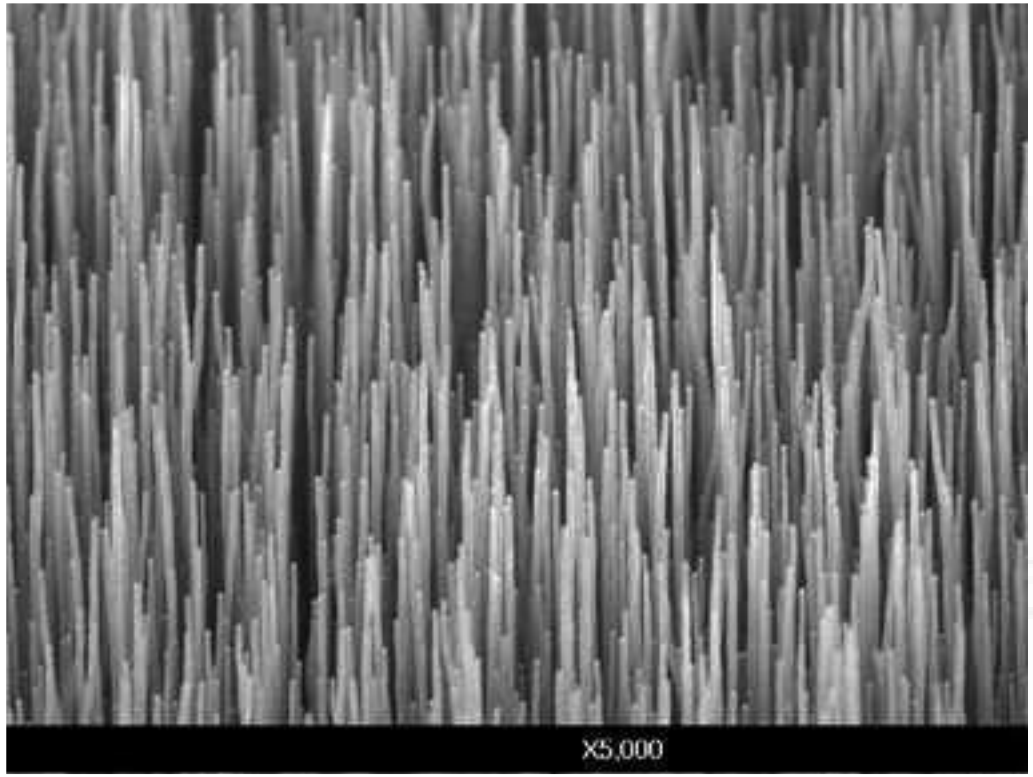

Multiwalled carbon nanotubes of an average diameter of 250 nm and a length of about 20 μm, grown on a stainless steel electrode.

Mechanical Structure

Step-1: the electrolyte droplet, the fixed electrode, and the moving electrode are placed inside the cavity in the SOIC chip

Step-2: A very thin aluminum cylinder with a height of approximately one-half that of the cavity is also inserted in the cavity.

The purpose of the cylinder is to act as a **contact terminal for the moving electrode.**

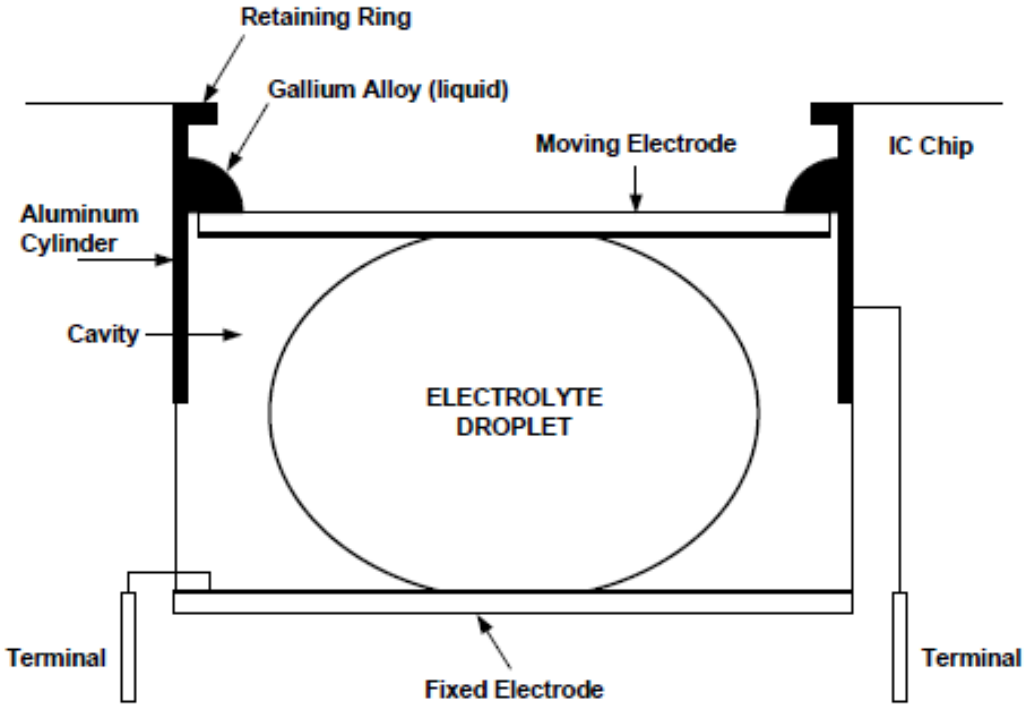

Mechanical Structure

Step-3: **“Liquid Metal”** is placed on top of the moving electrode and serves to establish **electrical contact between the electrode and the aluminum cylinder. The “LiquidMetal” is a gallium alloy that is normally liquid at temperatures above −20◦C**

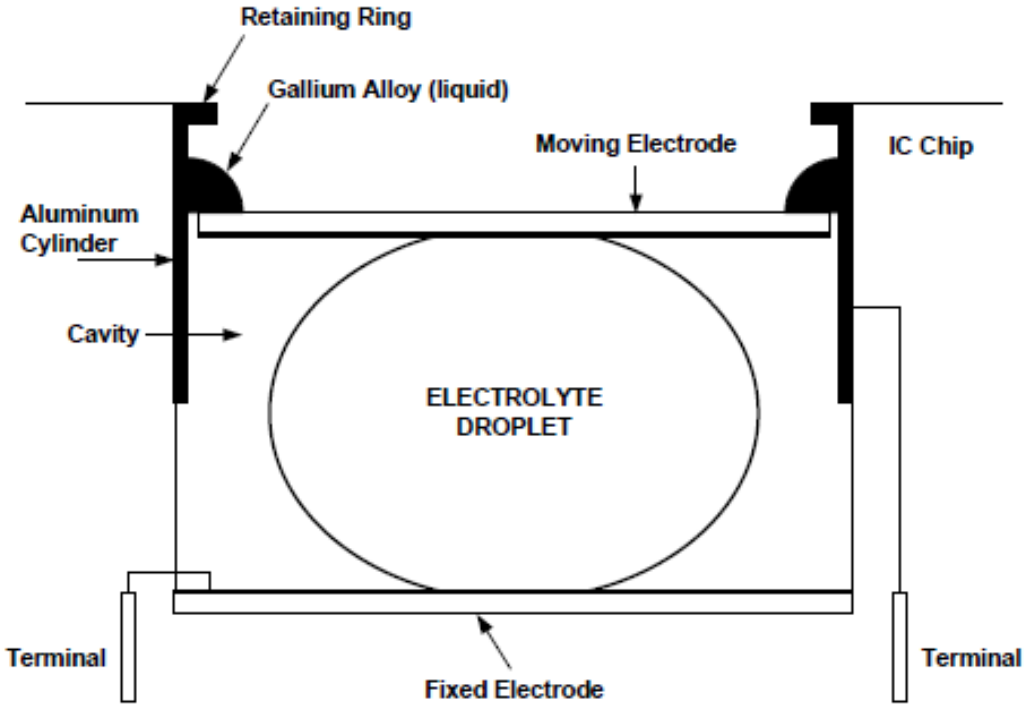

Step-4: A steel ring is placed on top of the cavity and serves to retain the moving electrode, and hence the electrolyte droplet, inside the cavity

Mechanical Structure

Step-5: The electrolyte used in the present application is **propylene carbonate (solvent)** in which an ionic salt is dissolved (a typical ultracapacitor electrolyte

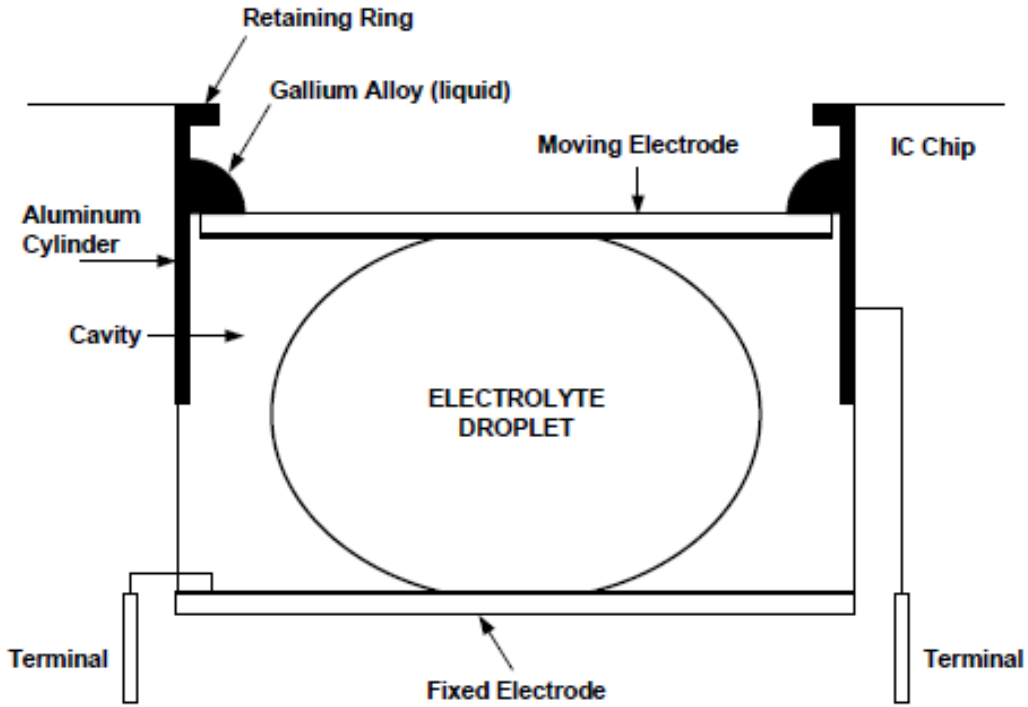

Observations

First: It is to be pointed out that propylene carbonate **has a boiling point of 240◦C.** Accordingly, any possible evaporation of the electrolyte will occur only at elevated temperatures. **The sensor was indeed tested at temperatures of up to 80◦C, and no evaporation of any kind was observed.**

Second: The second issue concerns the possible effect of the inclination angle on the measurement provided by the sensor. It is to be pointed out that the weight of the electrolyte droplet is only 5 mg, and hence the surface tension forces are far larger than the deformation forces that exist due to the weight.

Comparison of the new sensor to other known types of capacitive Acceleration sensors.

	Sensitivity	Dynamic Range	Size
New sensor	2.27 nF/g	2200 g	3 mm (dia) x 2 mm (h)
Other capacitive acceleration sensors	typically a few pF/g	typically a function of the size	few cm up to a few hundred cm (for each dimension)

Theory

For each CNT, the hydrophobic force (or force that repels the fluid away from the CNT) will be given by

$$F = 2\pi r\gamma\cos(180^\circ - \theta)$$

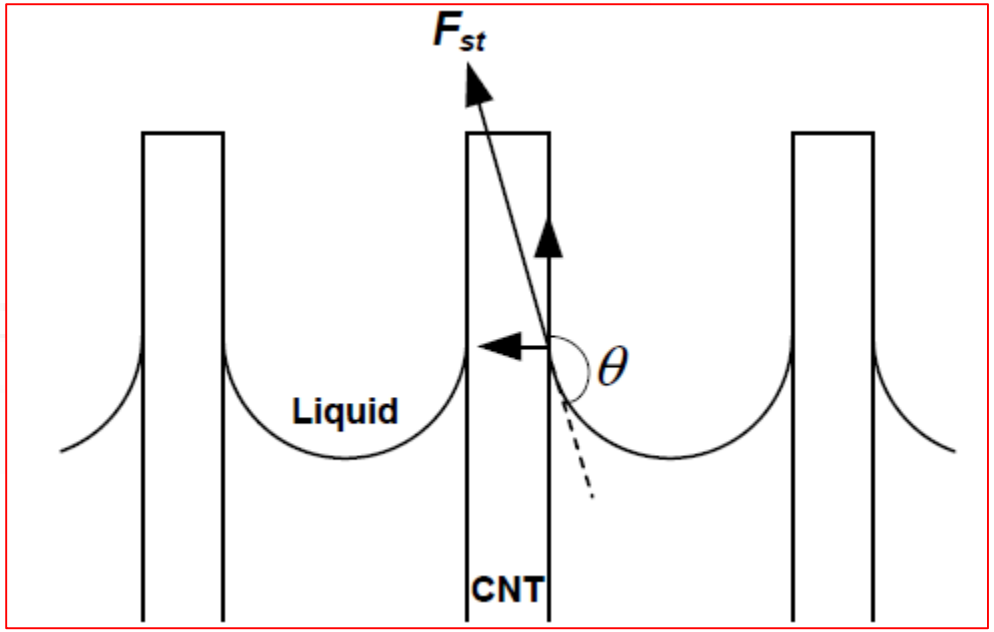

r is the radius of one CNT,
γ is the surface tension of the fluid,
θ is the liquid–solid contact angle, and the product
$2\pi r\gamma$ represents the surface tension force

Theory

Newtonian force $F = ma$ must be balanced by the total hydrophobic force, that is,

$$F_{total} = ma = 2\pi r N \gamma \cos(180^\circ - \theta)$$

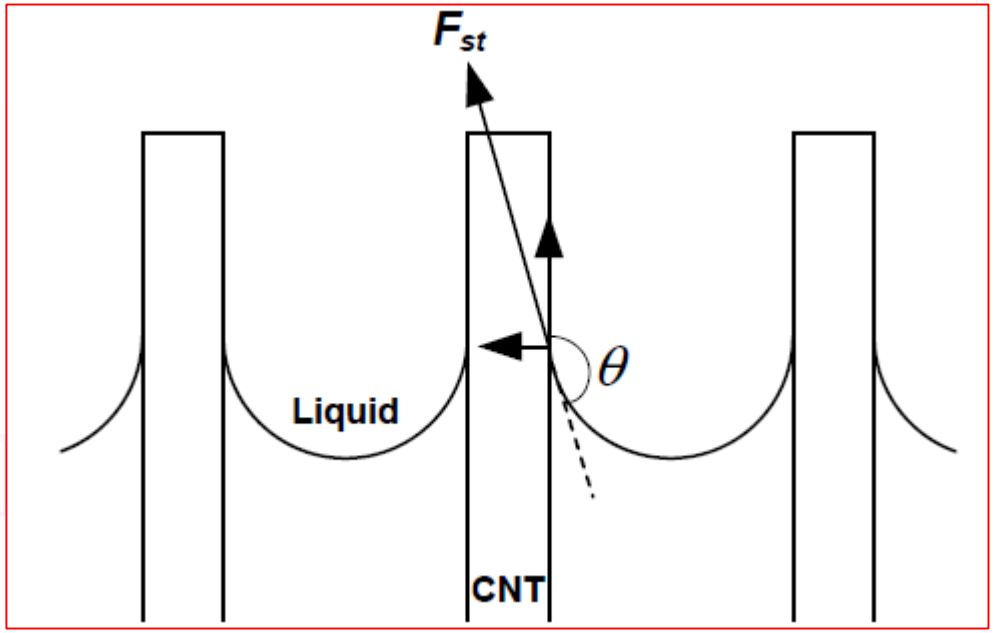

The capacitance of the electrode–electrolyte interface will be now given by

$$C = \frac{\varepsilon_0 \varepsilon_r A}{d}$$

$$A = 2\pi r \sum_{i=1}^{N} x_i$$

The surface area A of the CNTs where x_i is the immersion depth of any given CNT.

Structure

The total capacitance of the ultracapacitor is the series combination of the capacitances at the two interfaces $C1$ and $C2$.

$$C = \frac{\varepsilon_0}{d}\left(2\pi r \sum_{i=1}^{N} x_i\right)$$

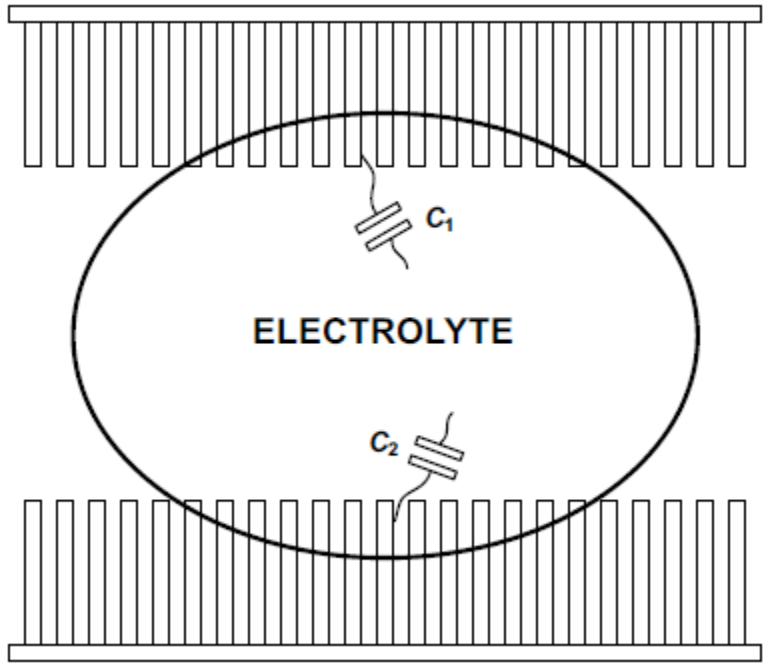

In general, C_2 will be larger than C_1, since the lower interface is acted upon by **both the upper electrode and the electrolyte droplet**

the series combination of C_1 and C_2 can be expressed as

$$C_{total} = K\frac{\varepsilon_0}{d}\left(2\pi r \sum_{i=1}^{N} x_i\right)$$

where *K* is a constant that ranges from 1 at very small accelerations (where $C_2 \gg C_1$)

0.5 at very high accelerations (where $C_2 \approx C_1$)

$$ma = N\gamma\cos(180^\circ - \theta)\left(\frac{dC_{total}}{K\varepsilon_0\sum_{i=1}^{N} x_i}\right)$$

$$a = -\frac{dN\gamma\cos\theta}{Km\varepsilon_0\sum_{i=1}^{N} x_i} C_{total}, \quad \theta > 90^\circ$$

Structure

Measurement of acceleration

Capacitance of the sensor during the acceleration pulse and calculating the value of the acceleration

Measured and theoretical acceleration in the range of 0.0002 g to 1 g as a function of the measured capacitance.

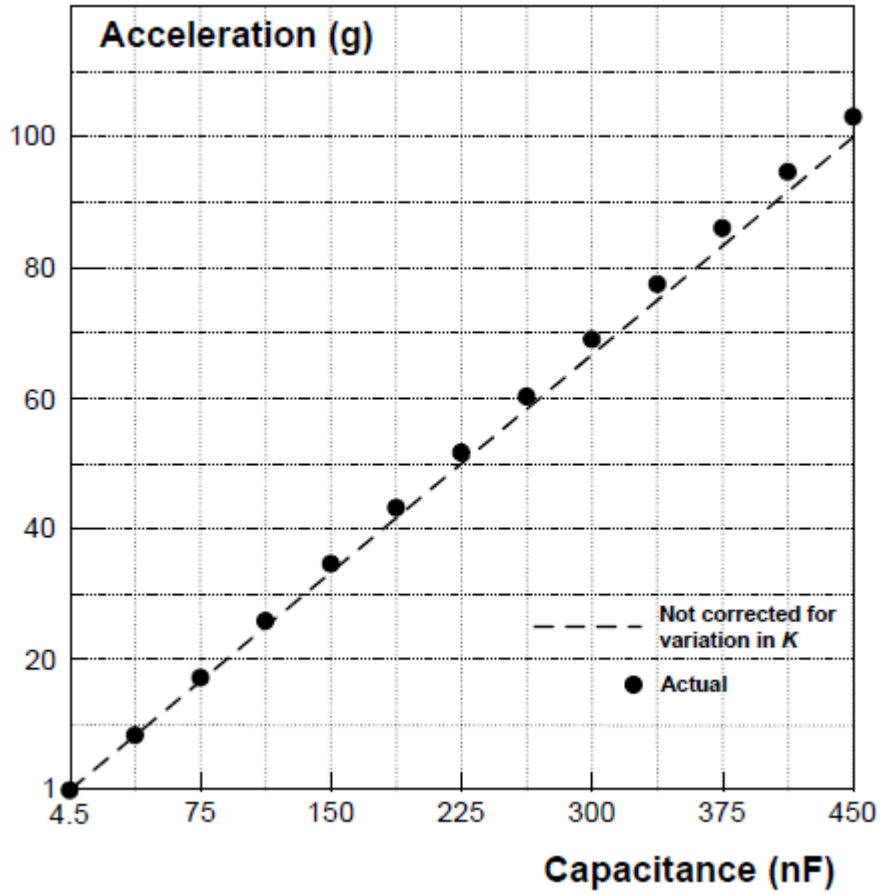

Structure

Measurement of acceleration

Capacitance of the sensor during the acceleration pulse and calculating the value of the acceleration

Acceleration in the range of 1 g to 100 g as a function of the measured capacitance.

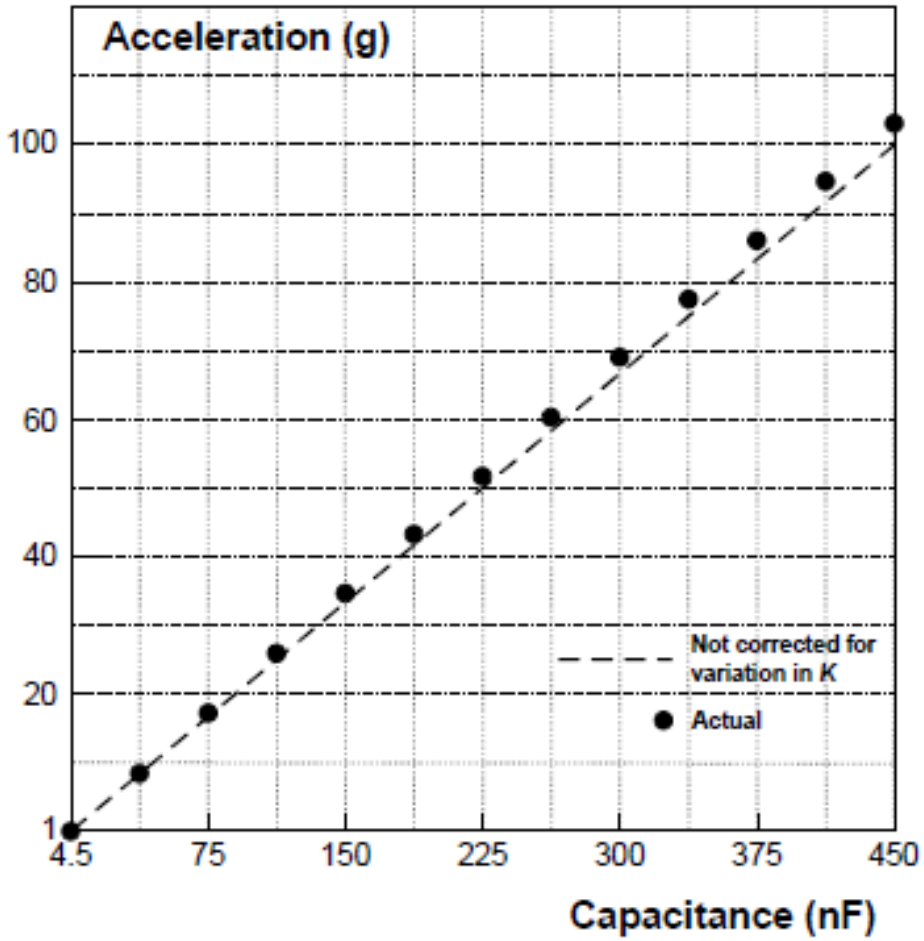

Structure

Block diagram of the interface circuit used for measuring the capacitance *C* of the sensor in real time.

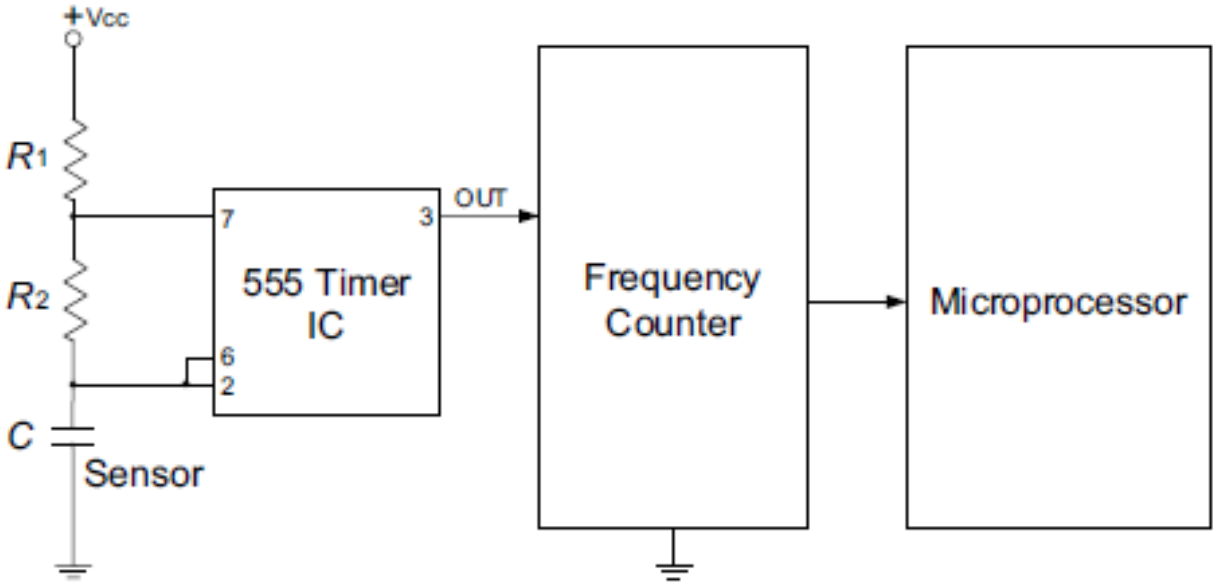

MEMS acceleration sensor described in this chapter has an ultra wide dynamic rage and high sensitivity. Specifically, the sensitivity is 2.27 nF/g,

The circuit board and the 0.45-caliber bullet that were used for testing the sensor at accelerations up to 2200 g.

Inference: Specifically, the sensitivity is 2.27 nF/g, and the dynamic range extends from **2×10−4 g to 2193 g**.

It will therefore be useful in a wide array of new applications, including **self-guided projectiles** and **autonomous surveillance aircraft**.

Other Motion and Acceleration Microsensors

Concept for a monolithic integration of pressure plus acceleration composite Tire Pressure Monitoring Sensor (TPMS) with a single-sided micromachining technology

Monolithic Tire Pressure Monitoring Sensor

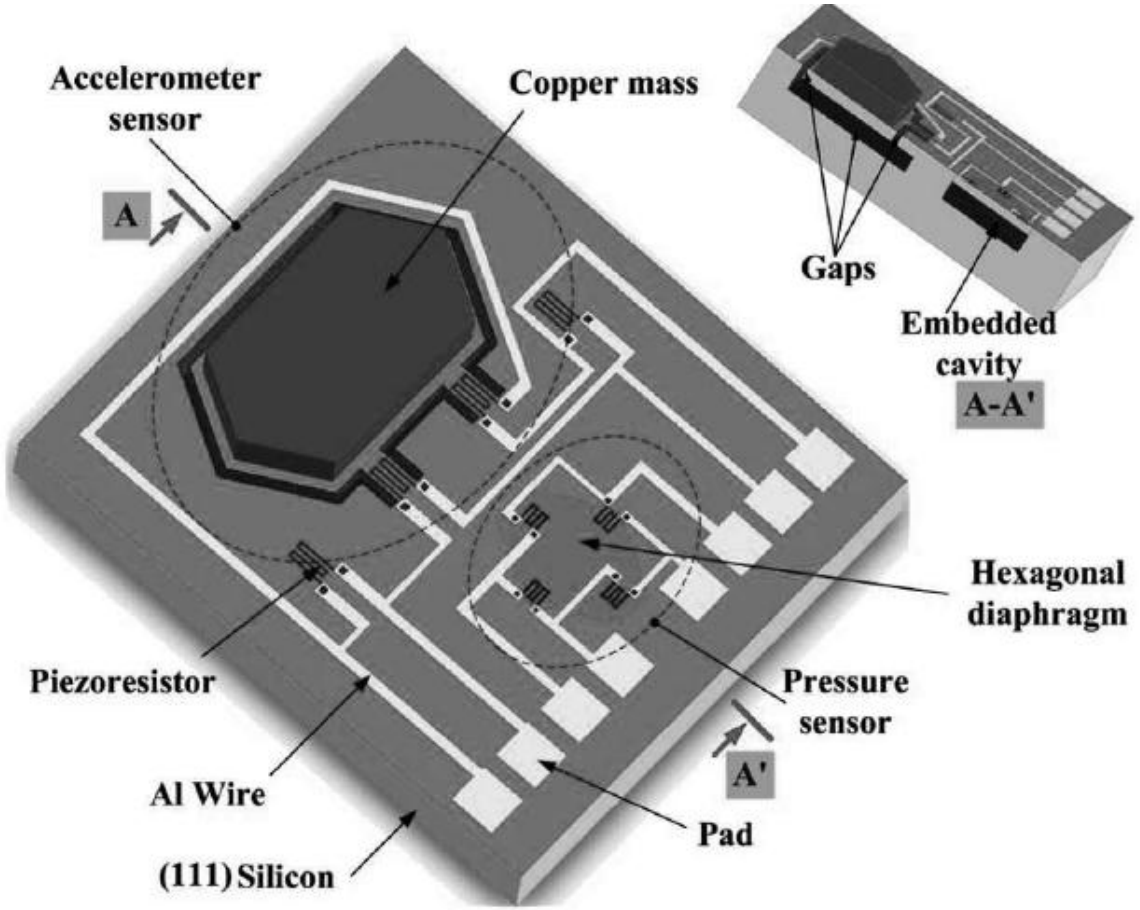

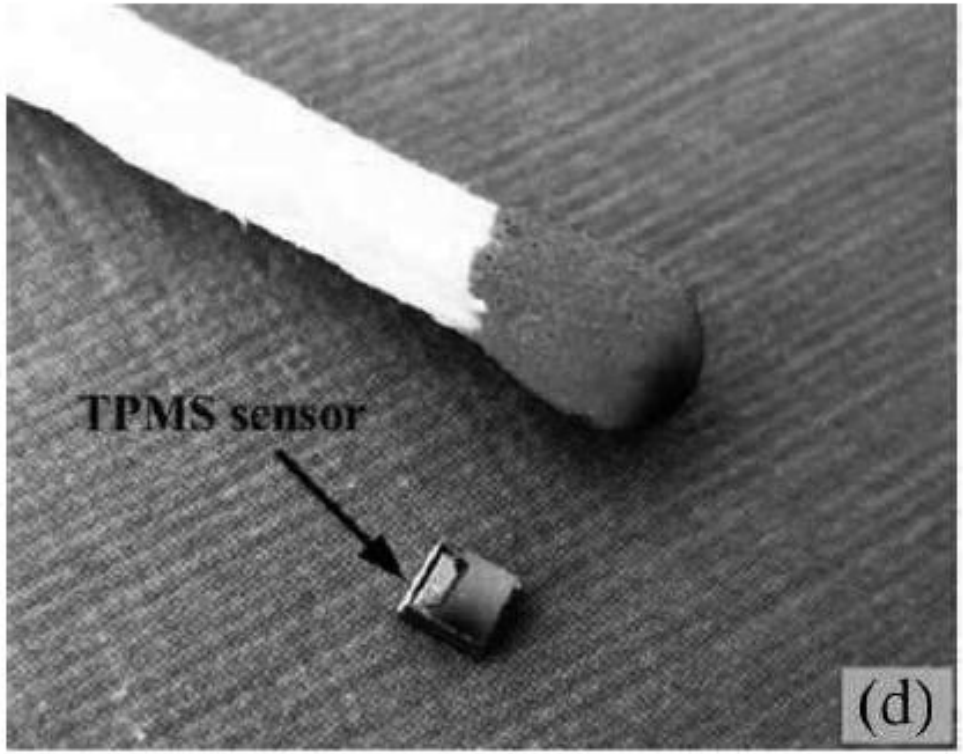

Quiz

1) True or false: applications such as self-guided projectiles require an acceleration sensor with a large dynamic range and high sensitivity

Quiz

2)Which scientific principle is behind the new ultraminiature, ultrasensitive acceleration sensor described in Module-2?

Ans: The use of a variable ultracapacitor.

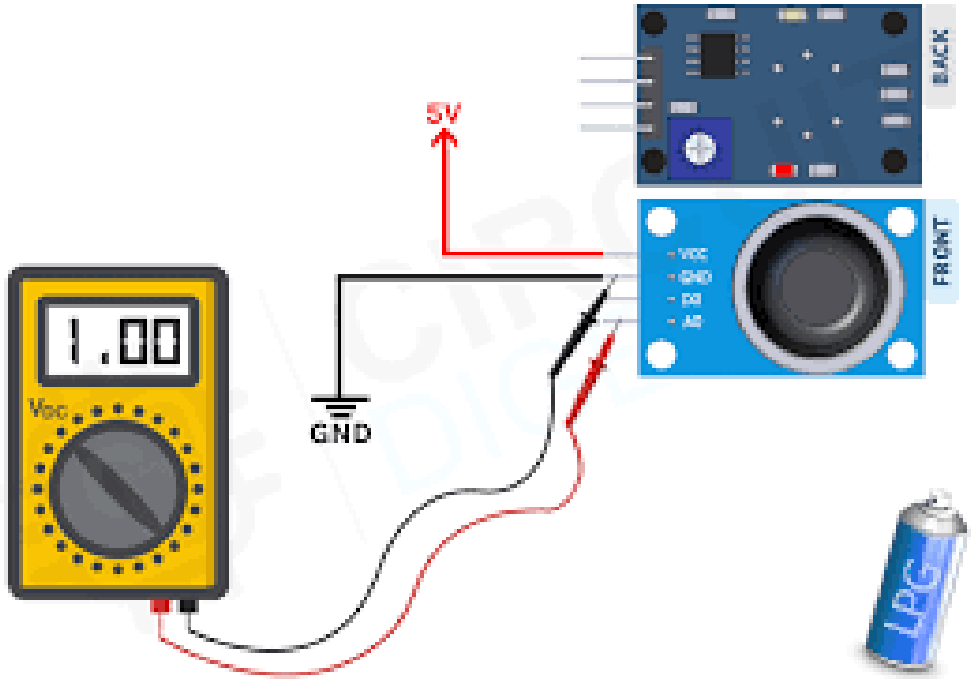
5V
GND
BACK
FRONT
VCC
GND
DO
AO
1.00
Vac
LPG

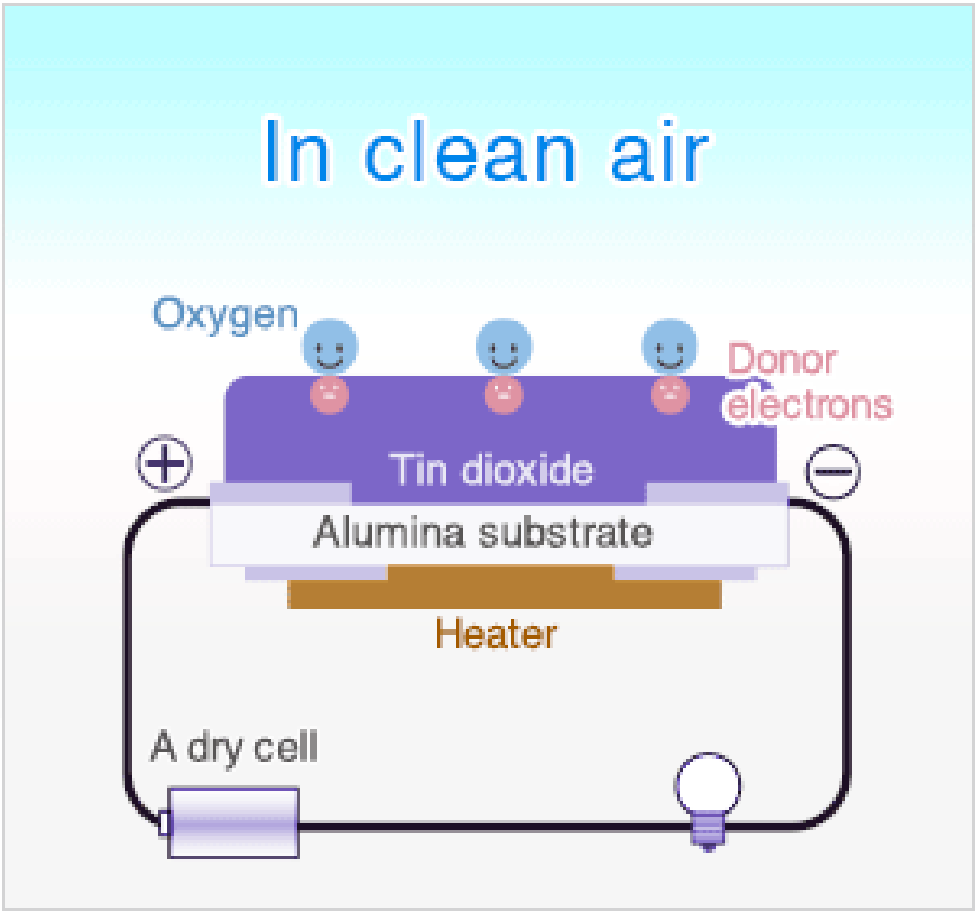
In clean air
Oxygen
Donor electrons
Tin dioxide
Alumina substrate
Heater
A dry cell

This section introduces a **carbon monoxide (CO) gas detector** that uses **gold nanoparticles** deposited on an array of **carbon nanotubes as a sensing element**, in addition to a smoke detector that achieves miniaturization by replacing a **bulky alpha particle detection chamber** with a silicon nanostructure

A CO Gas Sensor Based on Nanotechnology

Carbon monoxide (CO) detectors are used extensively in the **household** and the **industrial sector.**

Usually, a CO concentration in excess of 100 parts-per-million (ppm) is considered to be harmful for humans

To detect such a small concentration, detectors have traditionally been large devices.

The necessary **sensitivity** is achieved by using a **large electrochemical cell** or a group of heated semiconductor wires

Oxidation reaction of CO (to form CO_2) results in a small electric potential that can be detected

Step-1: Highly sensitive **CO gas sensor** that makes use of the **very high catalytic activity of gold nanoparticles** was introduced recently

Step-2: Gold nanoparticles are deposited on the surfaces of an array of carbon nanotubes (CNTs).

Step-3: The CO gas is transformed into CO_2 as it comes in contact with the nanoparticles, and **free electrons are released**

Step-4: The extra free electrons result in a measurable reduction in the resistivity of the CNT array.

The detector has proved to be very sensitive at room temperature to CO gas concentrations as low as 100 ppm.

It is characterized by a very small size and can be easily powered with a battery.

Fundamental principle of operation of the new CO detector.

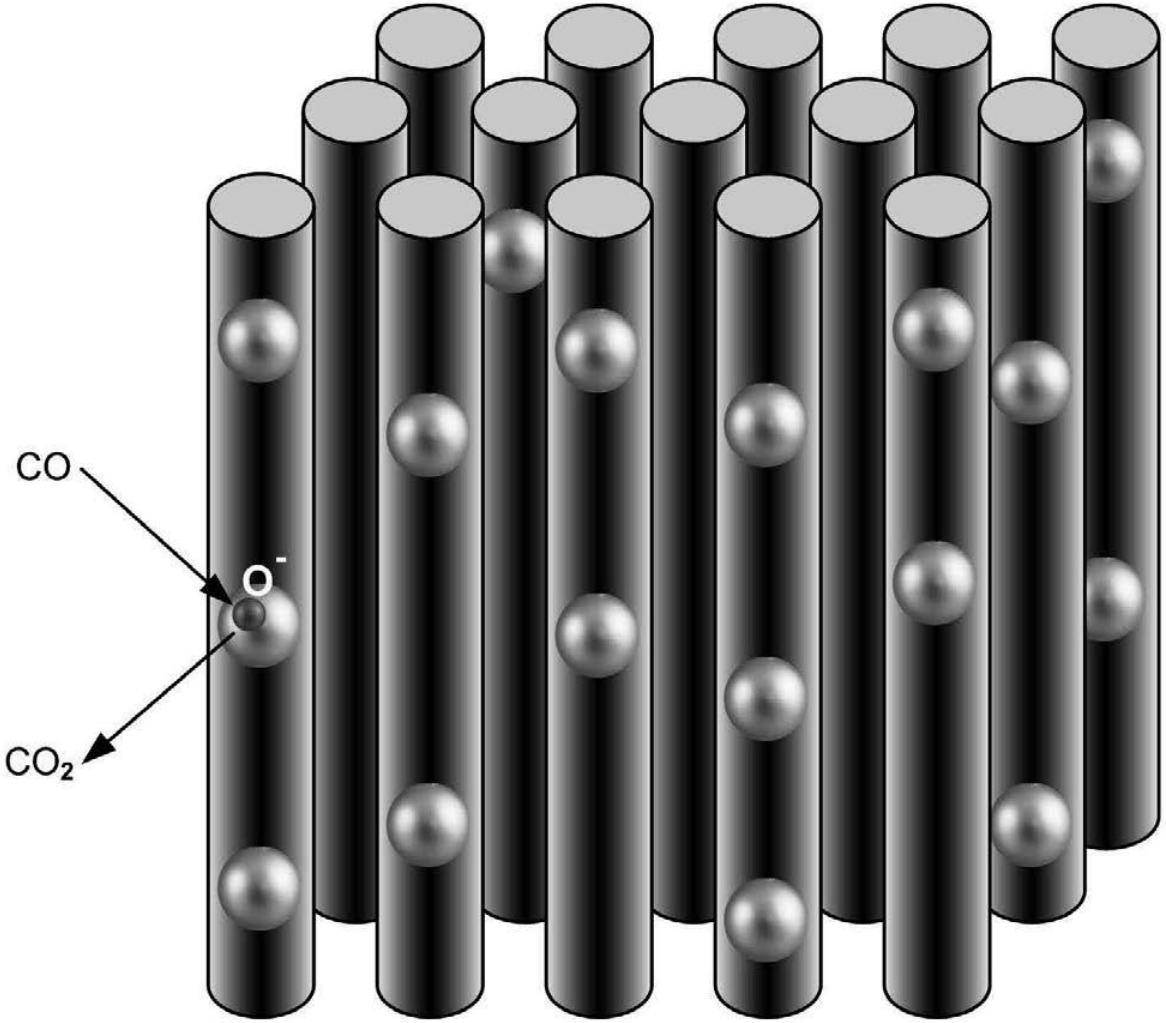

Structure

Step-1: The fundamental principle behind the new CO gas sensor is shown in Figure

Step-2: Gold nanoparticles are attached to an array of **multi walled carbon nanotubes**.

Step-3: Gold nanoparticles have a large affinity for oxygen, and oxygen molecules become adsorbed on the large surface presented by the nano particles, where they easily disassociate

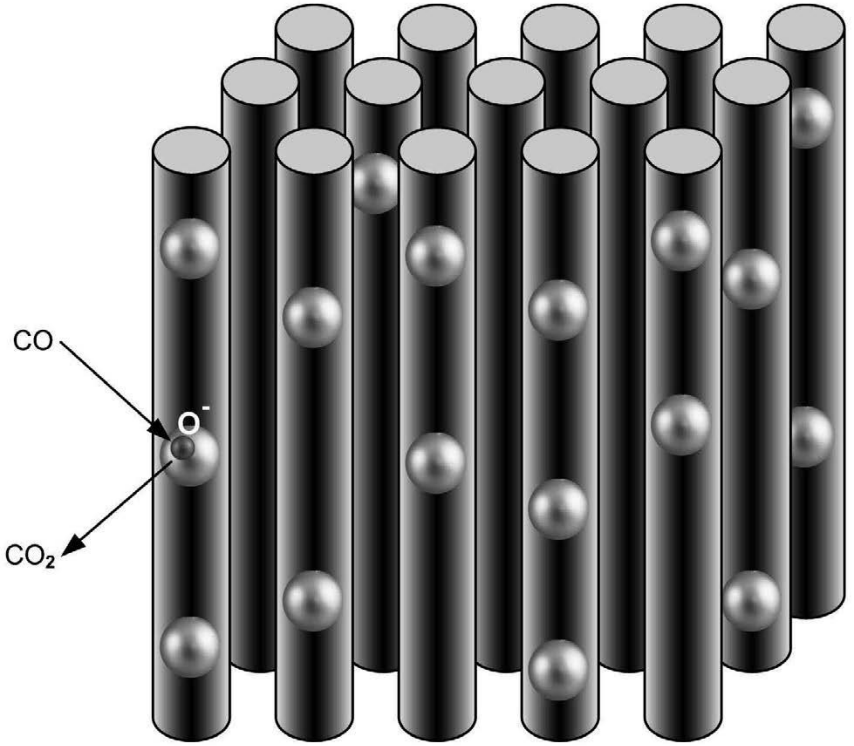

Structure

Step-4: CO, a reducing gas, easily combines with atomic (or molecular) oxygen and releases free electrons according to a well-known reaction.

Step-5: The presence of extra free electrons reduces the overall resistivity of the carbon nanotube array, which can be detected with an external circuit

$$2CO + O_2^- \rightarrow 2CO_2 + e^-$$
$$CO + O^- \rightarrow CO_2 + e^-$$

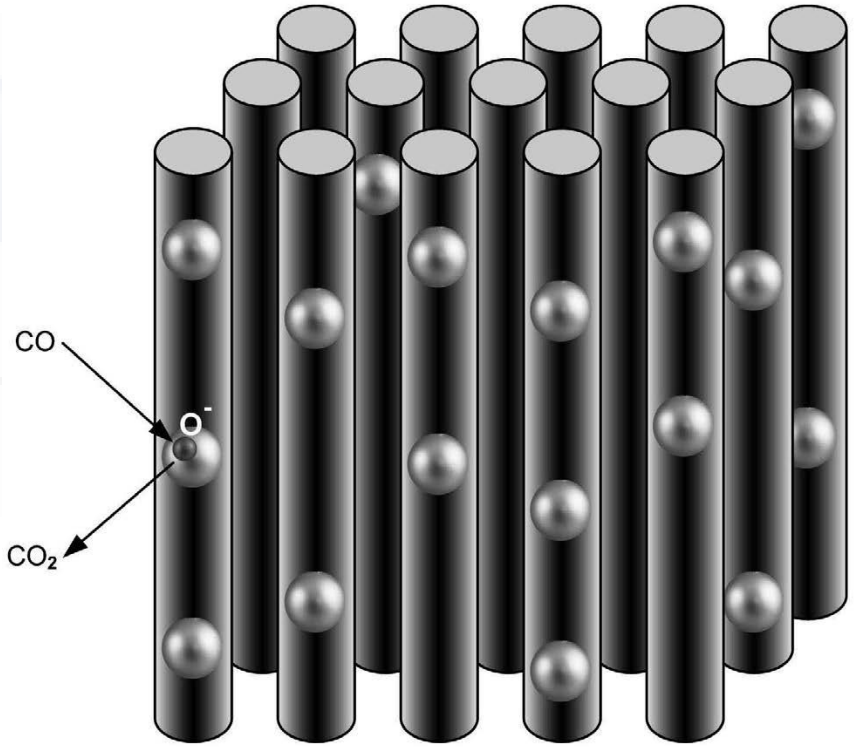

The miniature solid-state CO detector described in this section has the following characteristic advantages:

- **Sensitivity to CO concentrations** of less than 100 ppm at room temperature
- Can be battery operated, with a very long battery life (the power required is quite negligible when the audio alarm is not activated)
- Being a miniature detector, it can be placed virtually anywhere

Features of Sensor: **high sensitivity**, **relatively low cost**, **very small size**, and **operation at room temperature**.

Note: One ppm is equivalent to **1 milligram of something per liter of water (mg/l) or 1 milligram of something per kilogram soil (mg/kg)**.

Features of Sensor:

- **high sensitivity**,
- **relatively low cost**,
- **very small size**, and
- **operation at room temperature**.

Note: One ppm is equivalent to **1 milligram of something per liter of water (mg/l) or 1 milligram of something per kilogram soil (mg/kg)**.

Theory

The rate of the catalytic reactions can be described by the well-known **reaction rate equation**

$$-\frac{dP}{dt} = k_0 \exp\left(-\frac{E_a}{RT}\right) P^m$$

where ***P* is the partial gas pressure**,
***k*₀ is the pre-exponential factor**,
***E*ₐ is the activation energy,** and
***m* is the pseudo-kinetic order of the reaction** (the catalytic oxidation of CO by various catalysts shows a pseudo-kinetic order *m* that is usually 0 or 1)

A useful measure of the **performance of a gas sensor** is the **conversion percentage** (which, in this application, is the percentage of CO molecules that are converted to CO_2)

$$\alpha(t) = 1 - \frac{P(t)}{P_0}$$

where P_0 is the partial pressure of CO at time t =0

If m=1, the solution

$$P = P_0 \exp\left(-k_0 \exp\left(-\frac{E_a}{RT}\right) t\right), \qquad m = 1$$

$$\alpha = 1 - \exp\left(-k_0 \exp\left(-\frac{E_a}{RT}\right) t\right), \qquad m = 1$$

If $m = 0$

$$P = P_0 - k_0 \exp\left(-\frac{E_a}{RT}\right) t, \qquad m = 0$$

and α is found to be

$$\alpha = \frac{k_0}{P_0} \exp\left(-\frac{E_a}{RT}\right) t, \qquad m = 0$$

MOTION ALARM USING PIR SENSOR AND BC 547 TRANSISTOR

GAS SENSOR WITHOUT ARDUINO

Ultrasonic Object detection circuit without arduino

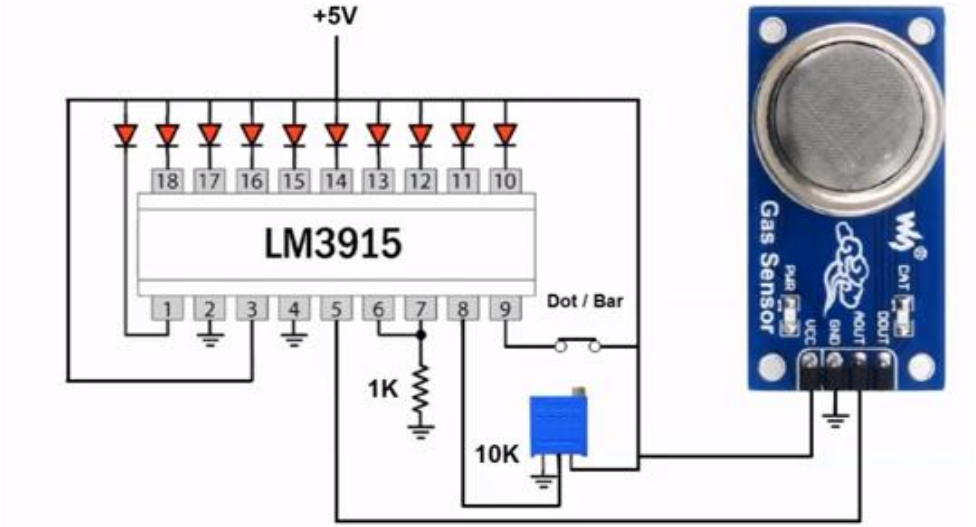

SEMmicrograph of gold nanoparticles deposited on multi-walled carbon nanotubes by direct redox reaction.

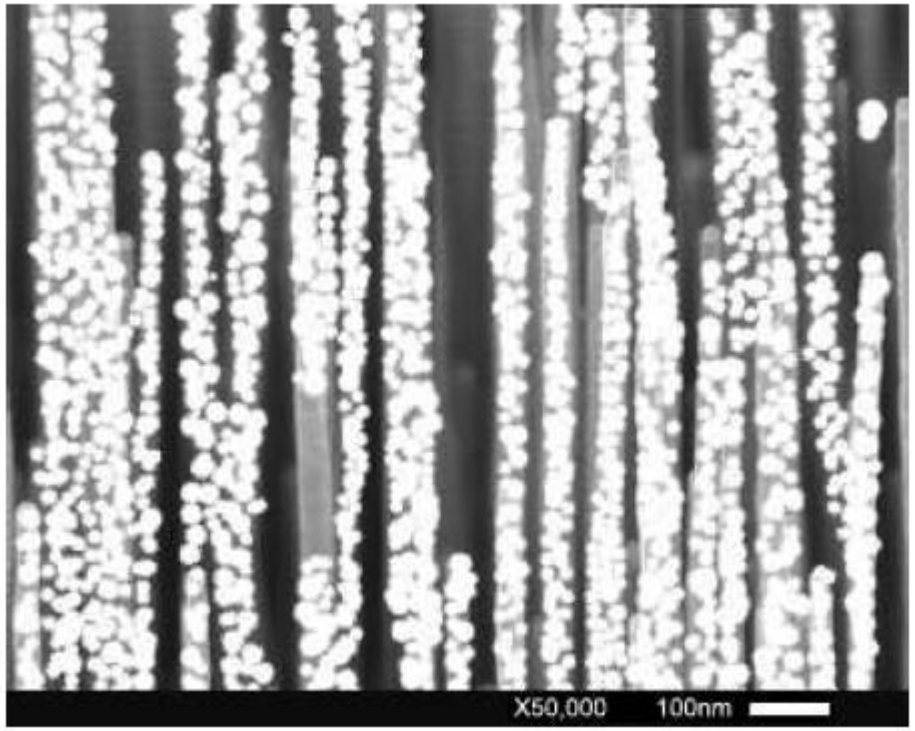

Experimental Results

Measurement of the resistance of the CNT array as a function of CO concentration:

- **Activity tests were performed** to determine the conversion percentage of the reaction as a function of time, and for **different values of temperature.**
- The sensor was placed inside a **small stainless steel reaction chamber** with a volume of 3cc/10ms, which is slightly larger than the volume of the sensor.
- The reaction chamber was in turn placed inside a **programmable temperature container.**
- CO gas mixed with air, at concentrations ranging from **100 ppm to 600 ppm,** was then pumped into the reaction chamber.

Experimental Results

Measurement of the resistance of the CNT array as a function of CO concentration:

- The rate of flow of the gas/air mixture was measured with a flowmeter and was adjusted to different values, the **maximum rate being 3 cc/10 ms** (hence, the measurements reported here have a resolution of 10 ms).

- The outlet of the chamber was connected to a **hydrocarbon gas analyzer** for monitoring the residual concentration of CO after passage through the sensor.

- It should be pointed out that the air used in the tests was ordinary room air that was **filtered with a charcoal filter** in order to **remove moisture and contaminants**

Conversion percentage as a function of time for temperatures ranging from 230 K to 300 K.

- Figure shows three different plots of the conversion percentage a as a function of time.
- The tests were conducted at temperatures of **300 K, 270 K, and 230 K.**
- The data in Figure is associated with a **CO concentration of 100 ppm**.

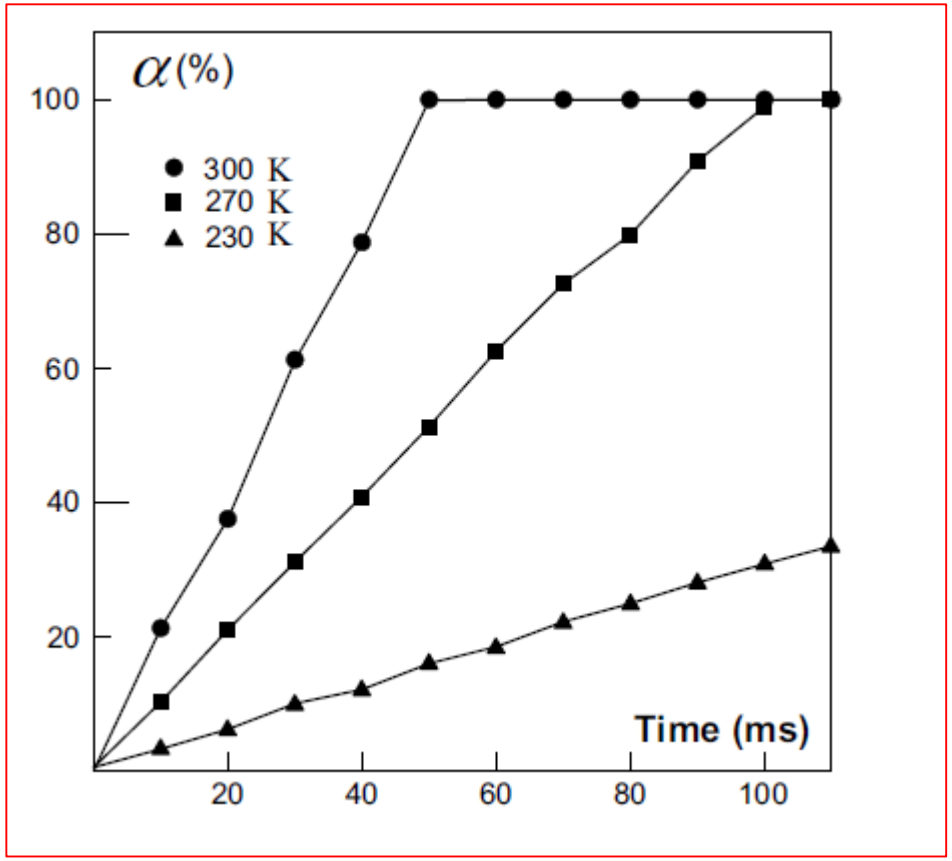

Conversion percentage as a function of time for temperatures ranging from 230 K to 300 K.

- It is clear that the plots in Figure show a **linear, rather than exponential, relationship**.
- Accordingly, the value of the constant ***m*** **is 0**.
- It is also clear that total conversion (from CO to CO_2) occurs very rapidly at room temperature (within 50 ms).

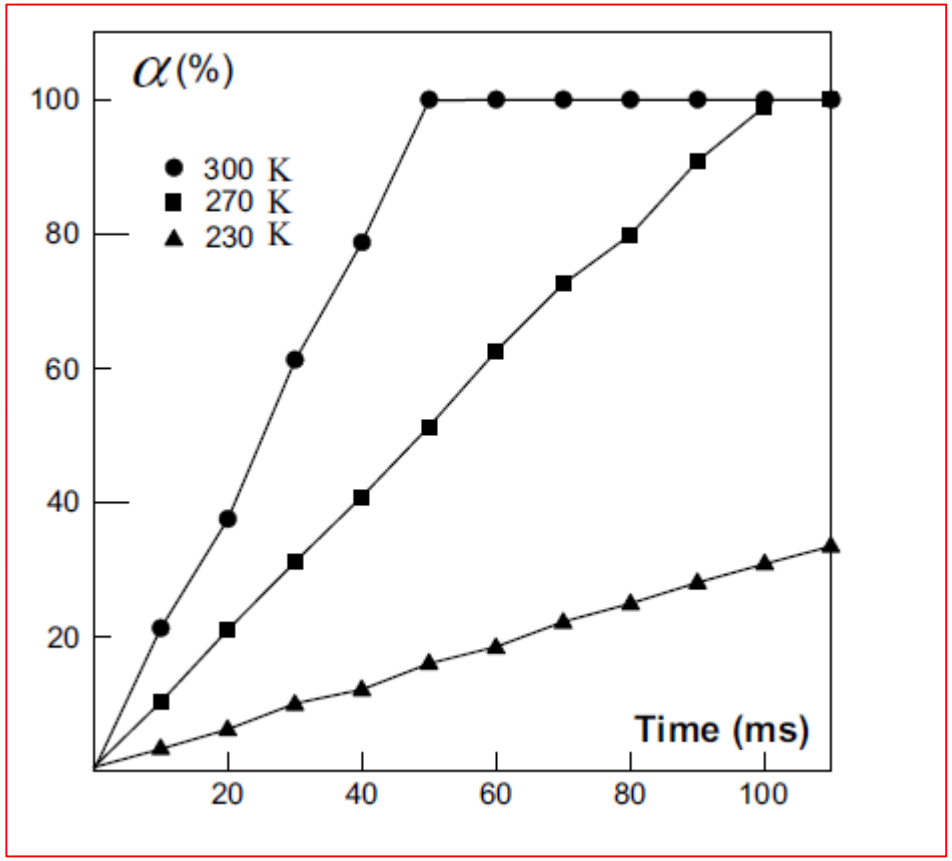

Conversion percentage as a function of time for temperatures ranging from 230 K to 300 K.

- The value of the slope for any of the linear plots in Figure 3.5 is given by
  $k0/P0 \exp(-Ea/RT)$.

- By comparing the slopes of two different plots, the value of the **ratio *k*0/*P*0** as well as of the activation energy ***Ea* can be determined.**

- From the data shown in the figure, *Ea* was estimated to be approximately 15 kJ.mol−1

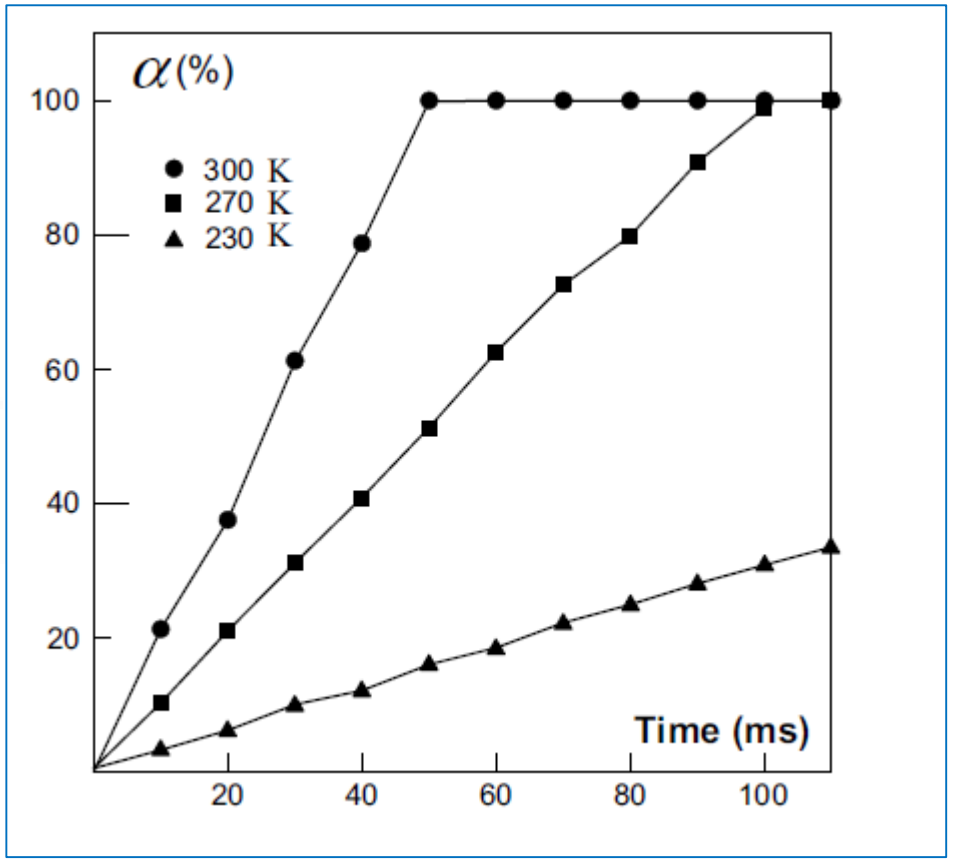

Conversion percentage as a function of time at a fixed temperature of 300 K and for 3 different CO gas concentrations.

Figure shows the **effect of the CO concentration in the gas/air mixture.**

The measurements in Figure were all taken at a **fixed temperature of 300 K.**

- Clearly, the effect of the concentration on the **performance of the sensor is minimal.**
- It can be noticed, however, that the reaction will require a slightly **longer time for completion at higher concentrations**, as it is obvious that more CO molecules will be competing for access to a fixed number of catalyst sites.

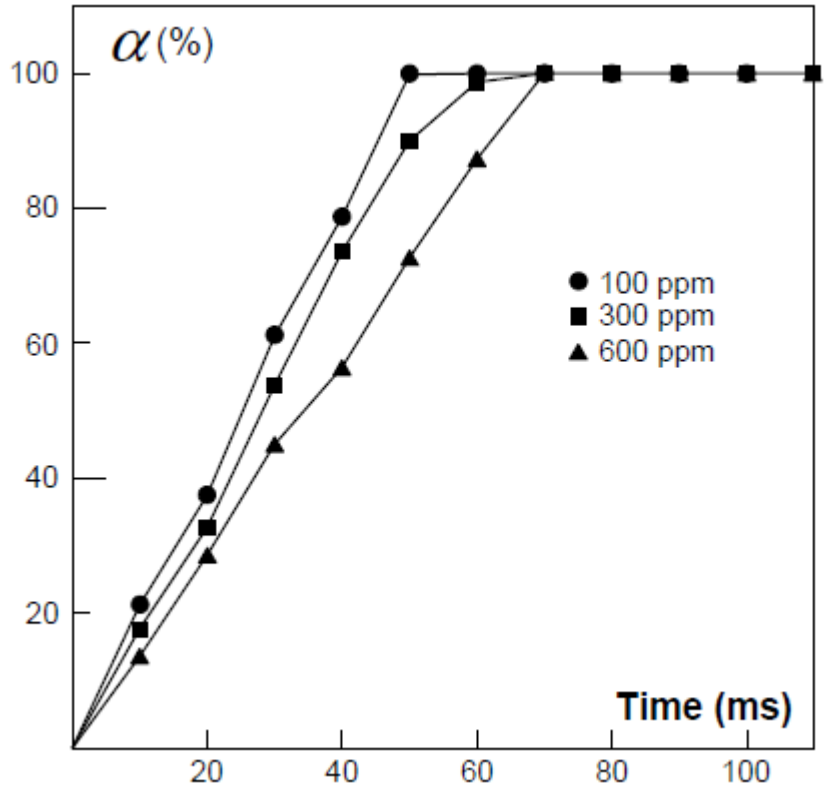

Measurement of the resistance of the CNT array as a function of CO concentration:

- The **resistance of the CNT array** was measured with a highly sensitive ohmmeter as the CO gas was repeatedly turned ON for a duration of 10 sec and OFF for a duration of 10 sec.

- Two multimeters were used to perform and verify the measurements:
  A specially modified Keithley model 610C multimeter, and **an Agilent model 34420A multimeter.**

Measurement of the resistance of the CNT array as a function of CO concentration:

- Both multimeters are capable of directly measuring a resistance of 100 nW or higher.
- For measurement of resistances that are less than 100 nW, however, the two mentioned multimeters were used in a 4-wire configuration, where one multimeter acts as a **current source** and the other as a **voltmeter**

Measurement of the resistance of the CNT array as a function of CO concentration:

Test-1: The first test was conducted with a CO gas concentration of 100 ppm.

The result is shown in Figure 1. As shown, the resistance drops from a nominal value of **0.5 mW to approximately 1 µW** when the gas is present. Hence, a good sensitivity to gas concentrations of 100 ppm or less is evident.

Test-2: The second test was conducted with a gas concentration of 600 ppm. The result is shown in Figure 2. It is evident that the response of the sensor is far greater, with the overall resistance dropping to an **average value of 10 nW**

Measurement of the resistance of the CNT array as a function of CO concentration:

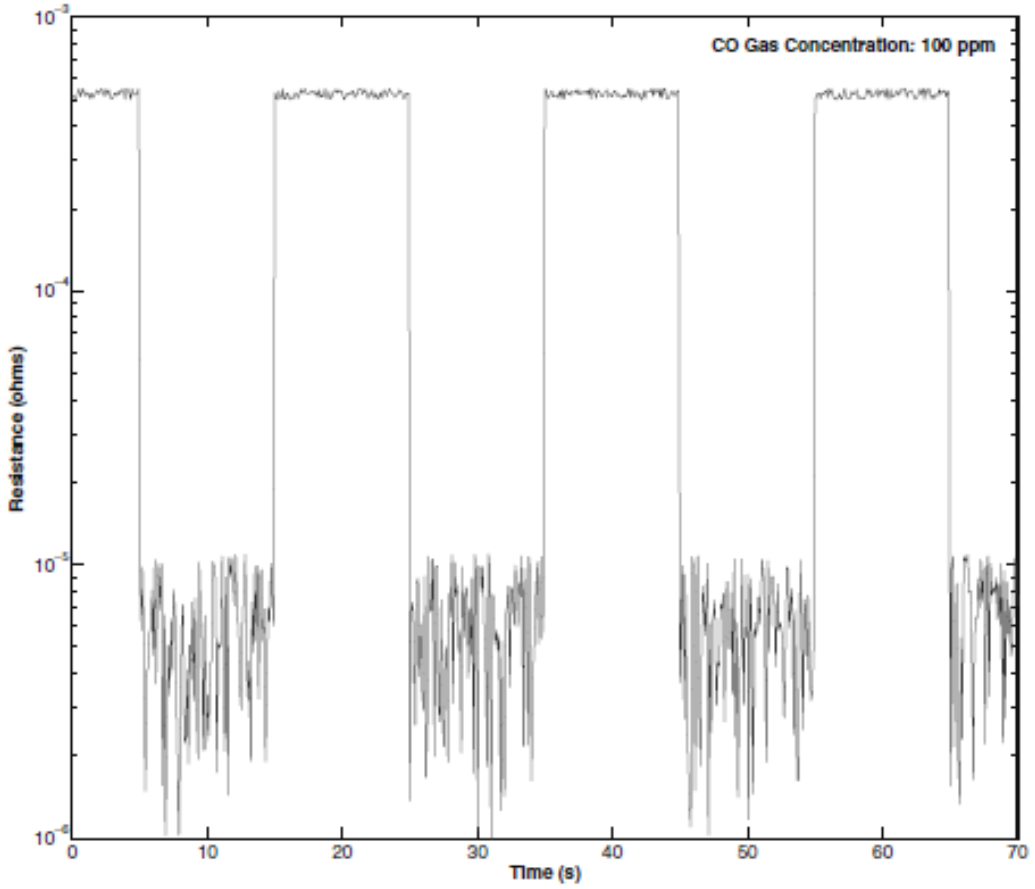

Resistance of the CNT array (log scale) as a function of time, as the CO gas (concentration: 100 ppm) is turned ON and OFF. The measurement was performed at room temperature. The nominal (upper) value of the resistance is 0.5 mW, and the lower value (measured when the gas was present) is approximately 1 μW.

Measurement of the resistance of the CNT array as a function of CO concentration:

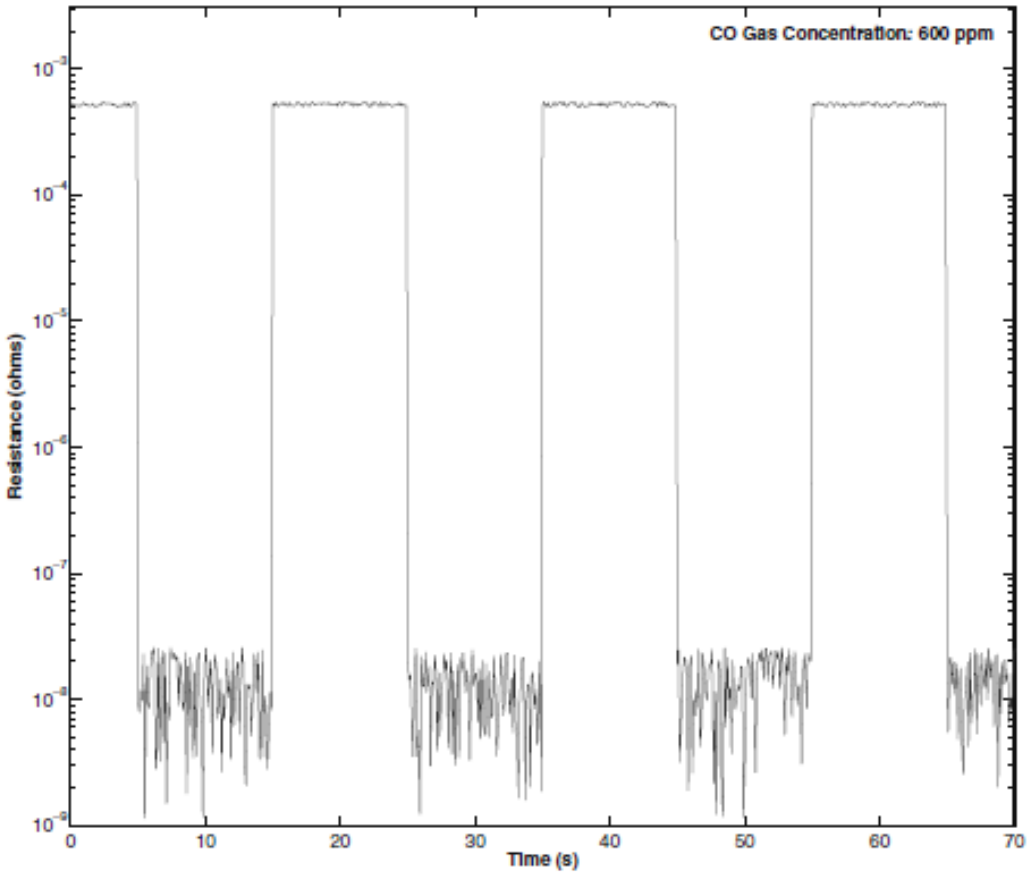

Resistance of the CNT array (log scale) as a function of time, as the CO gas (**concentration: 600 ppm**) is turned ON and OFF.

The measurement was performed at room temperature. The nominal (upper) value of the resistance is 0.5 mW, and the lower value (measured when the gas was present) has an average value of 10 nW.

Auxiliary Experimental Results

Effect of temperature on the performance of the sensor:

- The reaction rate (and hence the sensor's response) is quite acceptable at room temperature, but can be much worse at **substantially lower temperatures.**
- The sensor was also tested at elevated temperatures (up to 80°C), and the reaction rate was found to be generally higher at such temperatures.

Auxiliary Experimental Results

Effect of moisture on the performance of the sensor:

- Moisture was added to the gas/air mixture (by circulating the mixture through a valve-controlled container filled with distilled water), and the relative humidity in the mixture was monitored with a moisture sensor.
- Figure shows the result of a test that was conducted at room temperature and with a CO concentration of 100 ppm.
- As the figure shows, **the effect of moisture was negligible for the relative humidity (RH) range of 5% to 40%.**
- For the range of **RH from 40% to 80%, however, the reaction rate slowed** significantly. This can be understood on the basis of the fact that

Auxiliary Experimental Results

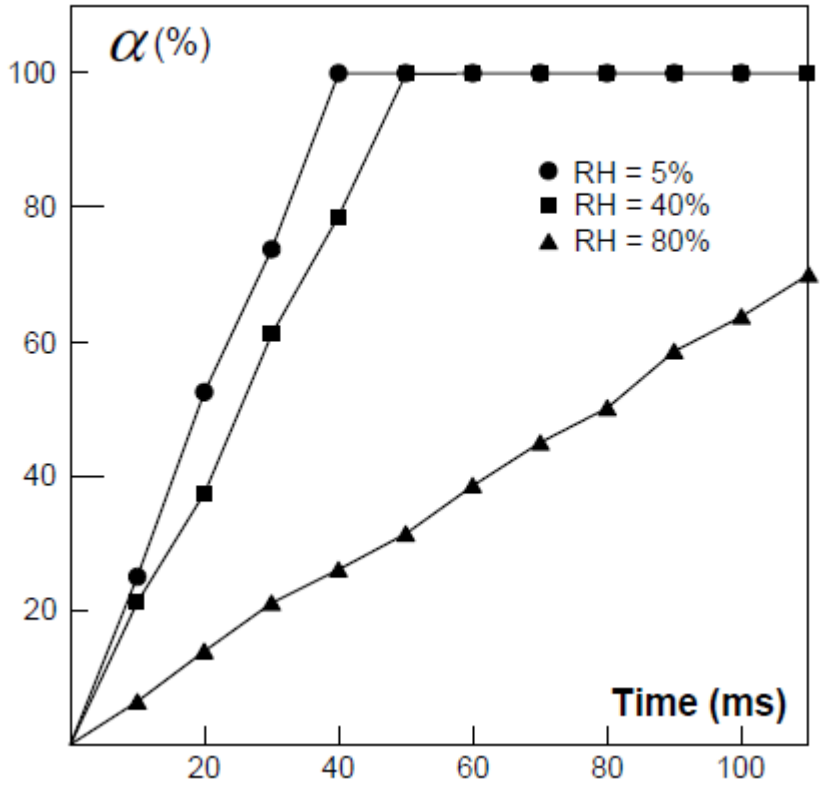

Effect of relative humidity on the reaction rate at roomtemperature (CO gas concentration = 100 ppm).

Smoke Detectors

Novel new smoke detector that is characterized by a **very small size** and **very high sensitivity**.

The new detector is fundamentally based on an **α -particle radiation** source like the well-known **α -particle smoke detector**;

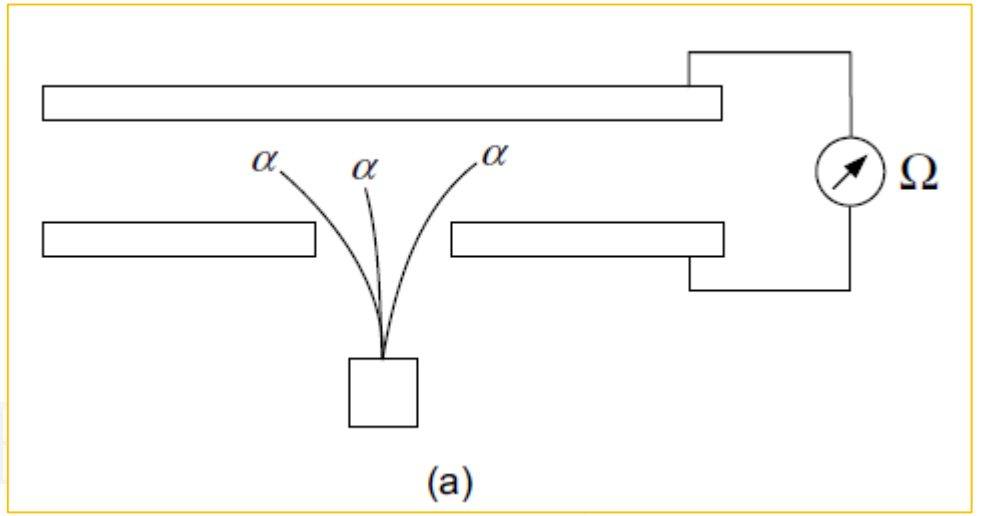

Smoke Detectors

Instead of utilizing the principle of ionization of the air, the α particles are made to **strike the gate of an n-channel MOSFET.**

This results in a **net positive charge** on the gate of the transistor.

(a) Principle of operation of the traditional α -particle smoke detector.

(b) Principle of operation of the new detector

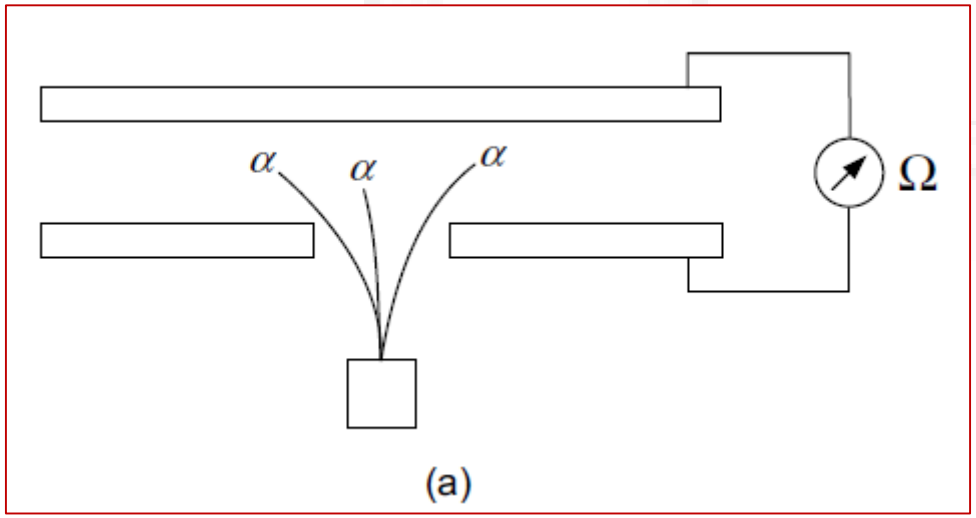

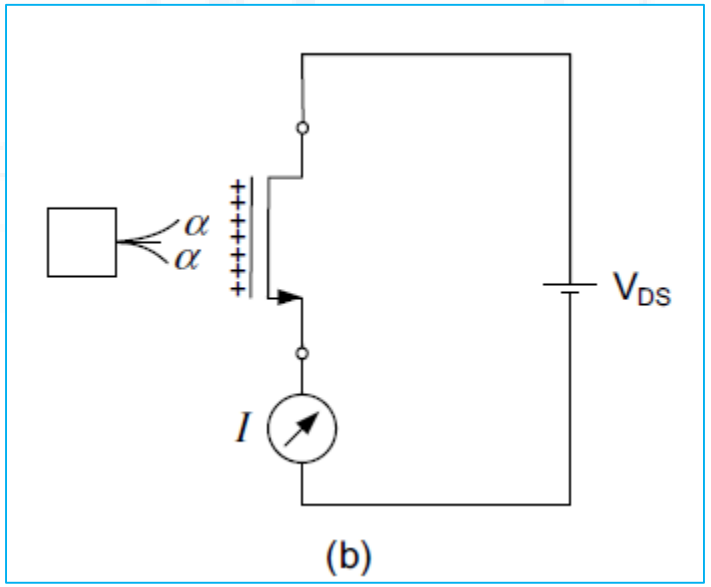

If particles of smoke enter the detector and screen the α particles, the **positive charge on the gate drops**, which leads to a reduced current or total cut-off of the MOSFET

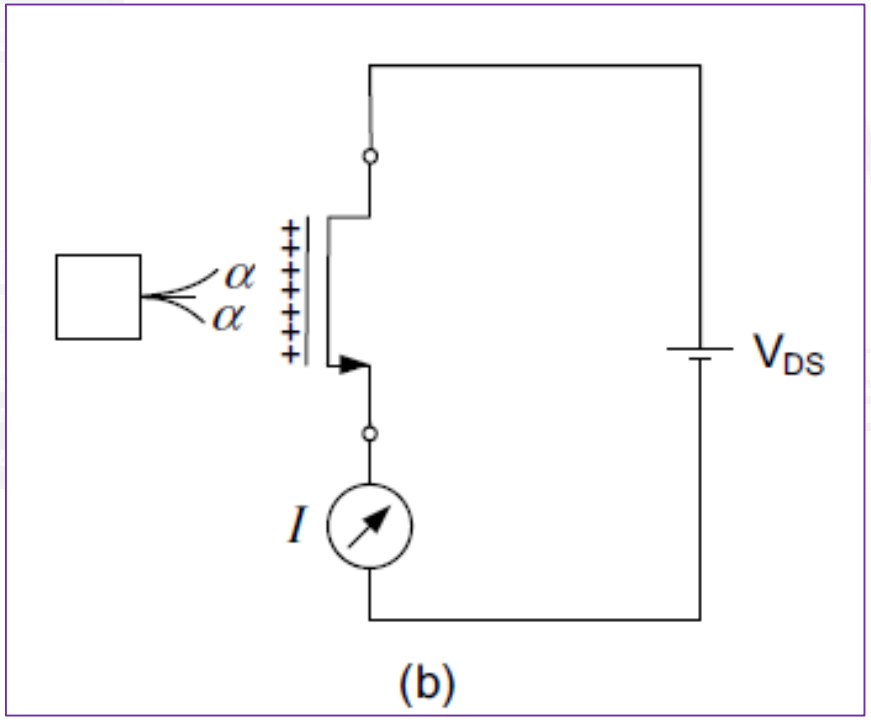

(b)

Structure

Step-1: Figure (a) shows the basic structure of that popular smoke detector: an α-particle emitter, which emits a particles into an ionization chamber that consists of **two metal electrodes separated by air**

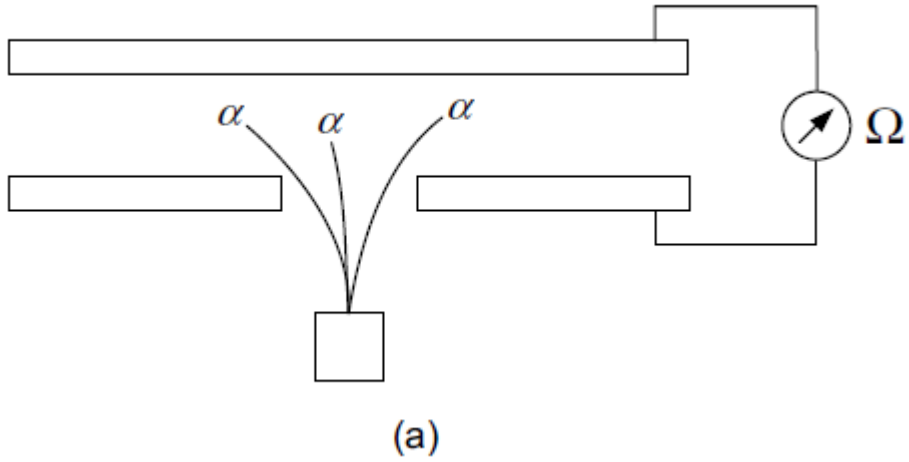

(a)

Step-2: The α particles ionize the air molecules, which results in the release of a large number of free electrons inside the chamber.

the resistivity of the air inside the chamber decreases, and a small current can be circulated between the two metal electrodes.

Step-3: When smoke particles (which contain a large number of carbon atoms), however, enter the chamber, they quickly attach to the α particles and hence reduce the degree of ionization of the air.

The **momentary increase in resistivity results in a lower current** between the electrodes, which can be detected with the external circuit.

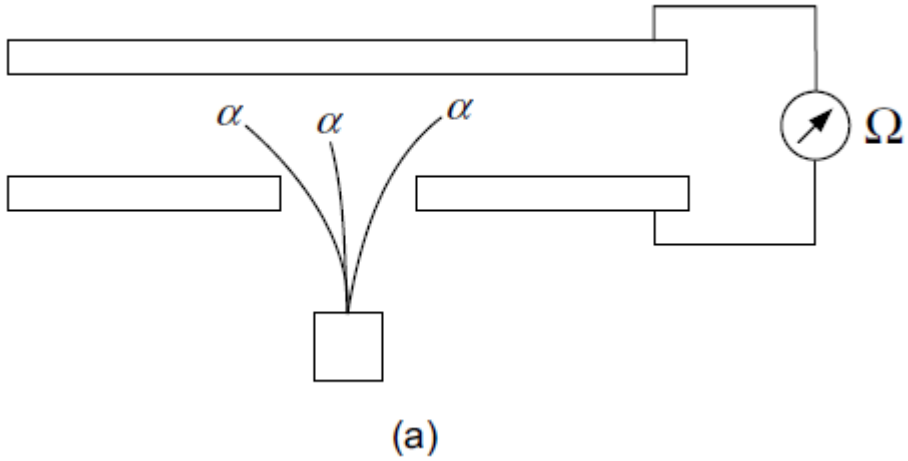

(a)

Note: Unfortunately, the **change in the resistivity of the air in the traditional smoke detector is quite small in practice,** which necessitates the use of a **large ionization chamber** and an elaborate external circuit to detect the small changes in resistivity that occur when smoke particles enter the detector

- In recent years, however, there has been an interest in a very small smoke detector that can be **hidden close to a passenger seat in an aircraft, train, or bus**

- Such a detector can be useful not only for detecting **cigarette smokers, but also for detecting potential terrorists** (who have attempted in recent years to use explosive/combustible materials inside public transportation systems).

Step-1: The α particles emitted from the α –particle source are made to strike directly the gate of an n-channel MOSFET transistor.

Step-2: The α particles, being **positively charged helium nuclei**, will deposit their positive charges on the gate.

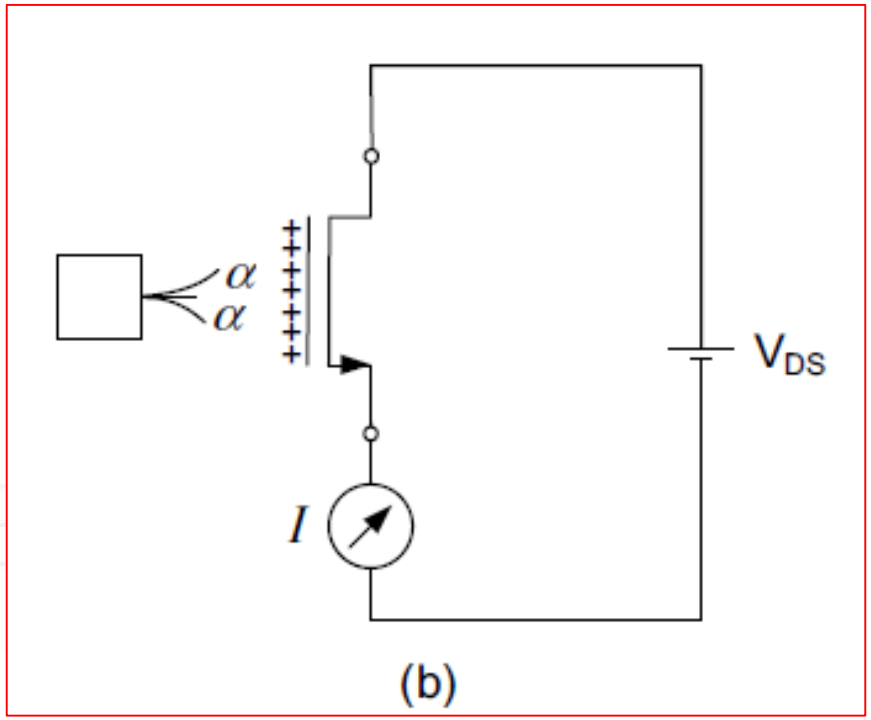

Step-3: The MOSFET is known to be highly sensitive to a charge on the gate and will immediately start conducting when the α particles reach the gate. **The current I through the MOSFET will be proportional to the charge on the gate**, and hence to the number of α particles reaching the gate.

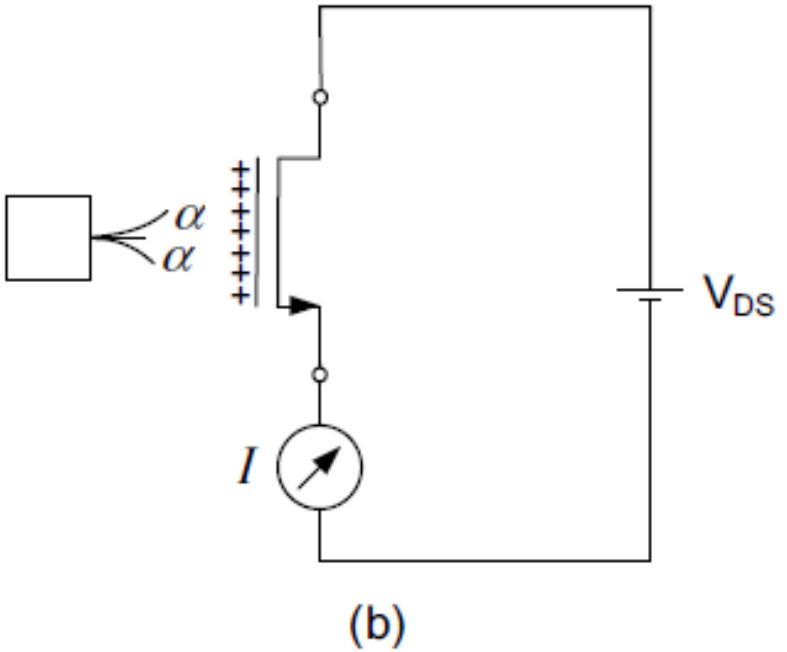

(b)

Step-4: **If smoke particles enter the detector and get attached to the α particles, a lower positive charge will be present on the gate**, which will lead to a lower current or total cut-off of the MOSFET

Qualitative Description of the Detector

Circuit used in the present prototype.

A DC buzzer can be connected to the output of the **driving transistor to obtain an audible alarm**.

Step-1:As shown, an α -particle source is arranged such that the emitted a particles strike a small plate that is directly connected to the gate of an n-channel, enhancement mode MOSFET.

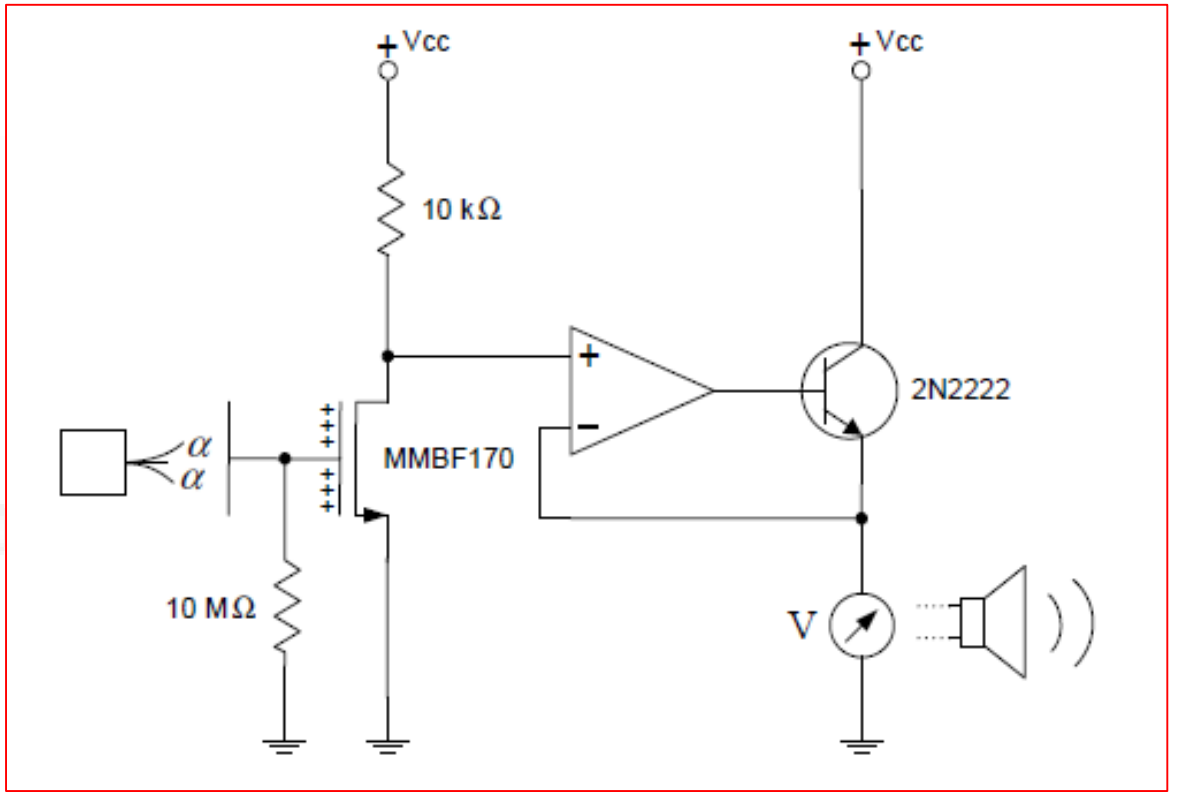

Qualitative Description of the Detector

Step-2:An optional 10 MΩ resistor can be connected to the gate, as shown, to drain the positive charge from the gate when the α particles are not present.

Step-3:The voltage on the drain terminal of the MOSFET is sensed with a voltage-follower. circuit consisting of a high-impedance op-amp and an NPN transistor. The purpose of the NPN transistor is to act as a load driver

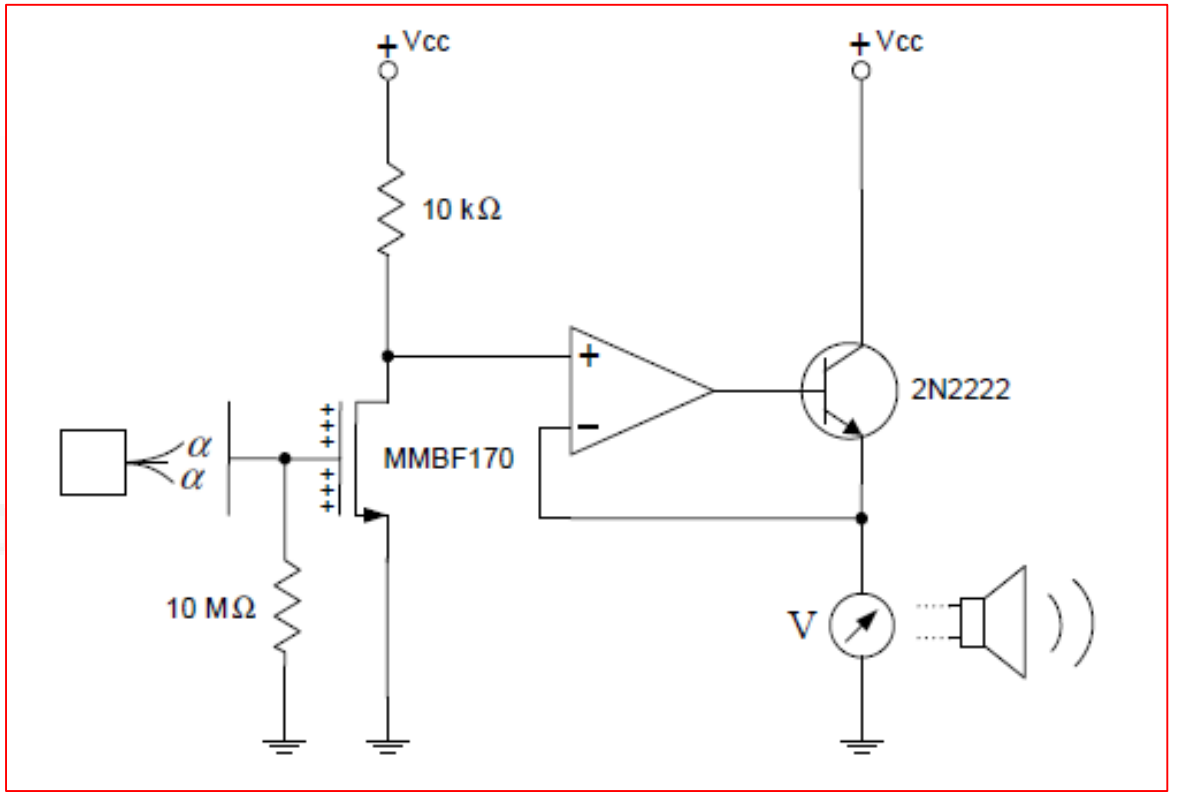

Step-4: When the a particles are striking the gate of the MOSFET and a positive charge is present, the MOSFET conducts and hence the **output voltage will be low.**

Step-5: If, however, the α particles are screened by the presence of smoke and no positive charge is present on the gate, the MOSFET shuts off.

But since the input to the op-amp is connected to a pull-up resistor, the **output voltage in that case will be high**

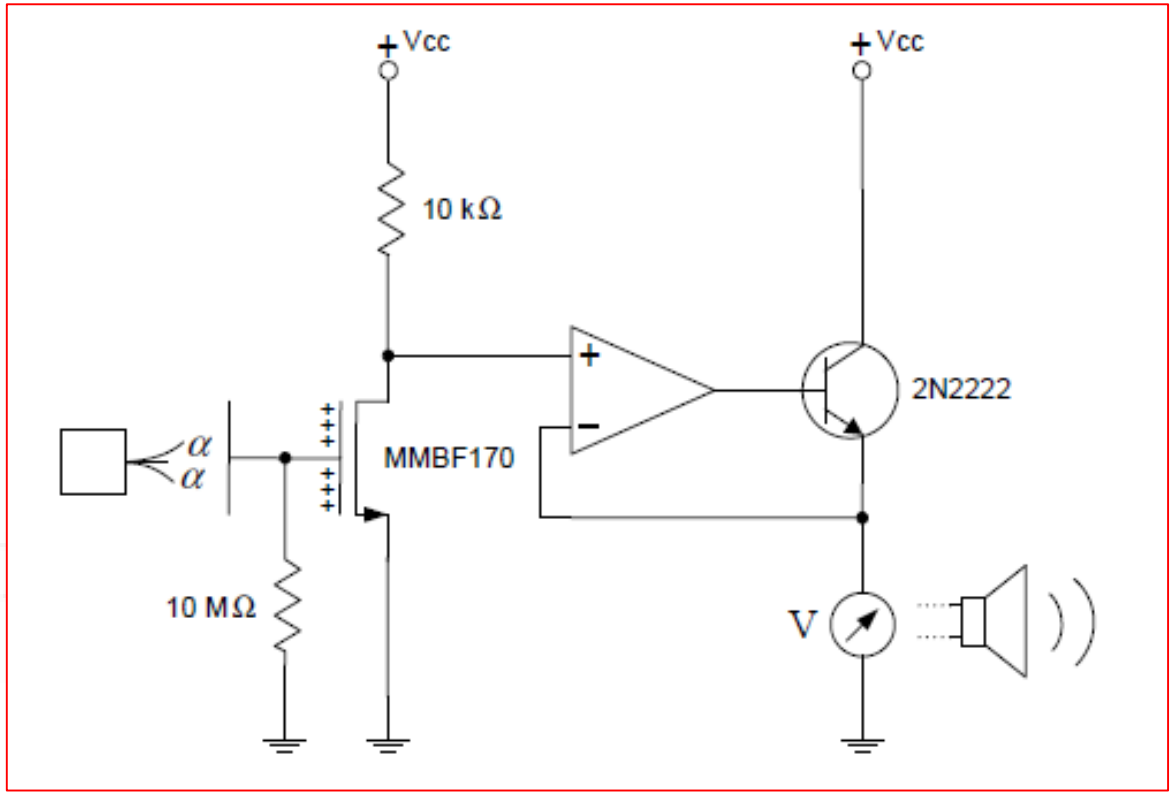

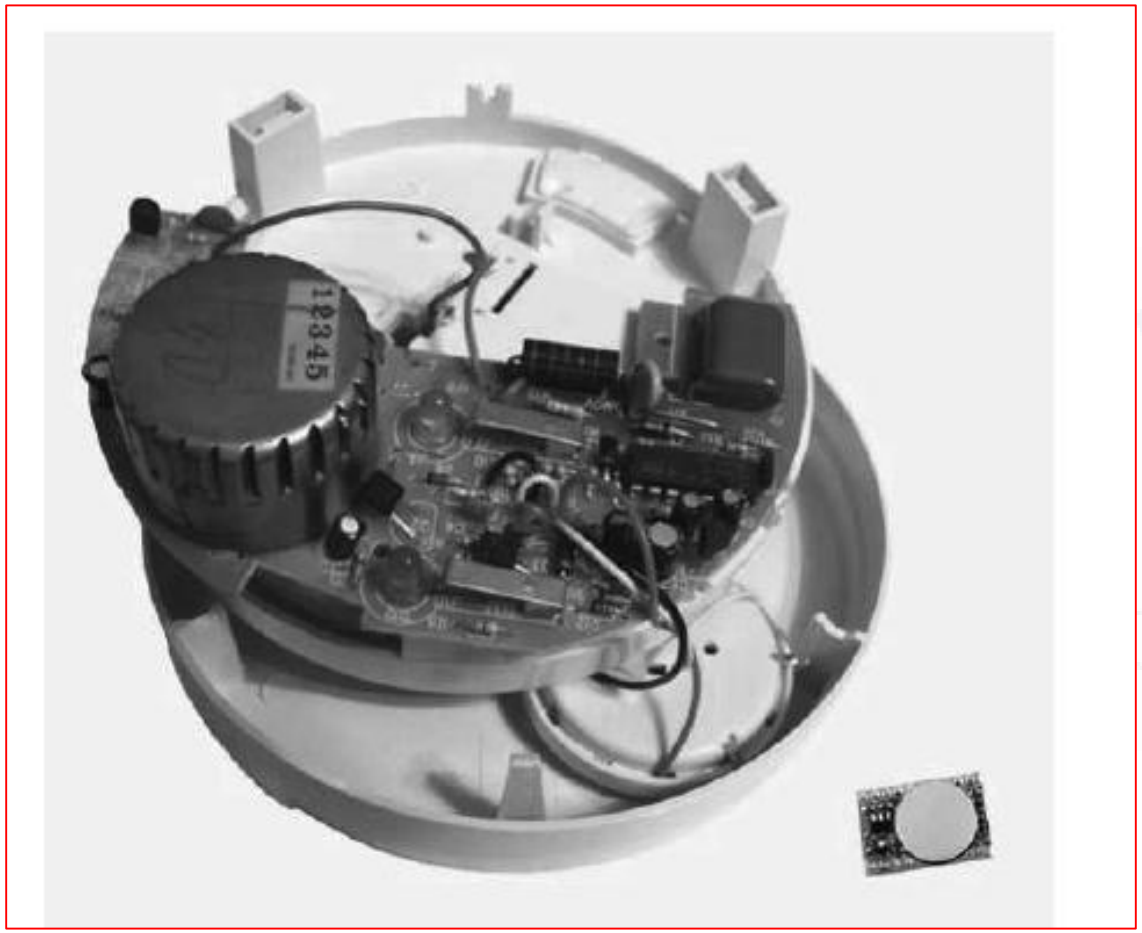

Photograph of the new detector

THANK YOU